A COMPILATION AND ANALYSIS OF INFORMATION CONCERNING THE GREENHOUSE EFFECT AND GLOBAL WARMING

Pablo Provecho Mosquera

Faculty of Sea and Environmental Sciences. University of Cadiz, Spain

pablo.provechomosquera@alum.uca.es

Introduction

One of the first mentions of global warming and the greenhouse effect was made by the celebrated Swedish chemistry and physics researcher Svante August Arrhénius (1859-1927). In those times, he already believed that the large amounts of fossil fuels, mainly coal, that were being burned in the industrialised countries were increasing the CO_2 concentration in the atmosphere. He also said that an increase of 100% in the CO_2 may cause an average warming of 4-6ºC in the atmosphere. Curiously, he believed that this greenhouse effect, produced by the human activity, would be a technical solution against another ice age in the future. Anyway, he was the first one to establish a relation between the fossil fuels burning and the climate changes.

Only after the Second World War could long term CO_2 measurements be started and it was discovered that the carbon dioxide concentration rose from 275 ppmv before the industrial revolution to 361 ppmv in 1996. Also, the methane (the third responsible greenhouse

effect gas after water vapour and carbon dioxide) levels were duplicated in the last hundred years (IPCC 2001).

The physical phenomenon of greenhouse effect is an easy topic to be described and understood. However, nowadays, the greenhouse effect is automatically associated with another phenomenon, global warming, and it is again associated with human's activities, but, is all of this true?

Are humans causing global warming?

Is the global warming true?

Can we do something if it is caused by ourselves?

The aim of the study was to make an attempt to answer the above questions. The main problem is that the same data, the same historic register, the same observation, can be interpreted in totally different ways (even the opposite) by ones or another's. This problem is amplified mainly by politicians, ecologists and the mass media, so the population can not reach the truth easily. One of the biggest problems is that this is not only a scientific topic (in that case, we can easily deal with it), but is also an economic, political and social problem because of the enormous implications to one side or the other. For these reasons most of the citizens can not know the truth, because they can not analyse the data by themselves so they can only chose between two "prefabricated theories".

Discussion of the topic

Physical description of the studied phenomenons: atmosphere, greenhouse effect and global warming

The main components are nitrogen (78%), oxygen (21%), and little amounts of some other gases such as water vapour (0,002%), carbon dioxide, methane, NO_x, CO, SO_2, or some other trace (noble) gases. Even if the amount of some compounds is very small, all of them are very important because every one can absorb and reflect some specific wave lengths. For example, ozone absorbs among others ultra violet radiation in the stratosphere. Water vapour and carbon dioxide absorb visible light and infrared.

Solar radiation

Practically, all the energy in the Earth comes from the sun (if we forget the internal heat and some deep radioactive process in the Earths crust). That energy comes in way of electromagnetic radiation, mainly with a wave length between 200 and 400 nanometres.

The total energy on the top of the atmosphere -during special assumptions- coming from the sun is called “solar constant”. If we do not take care about the short time little oscillations in orbital parameters and solar activity, we can consider it as a constant (Fig. 1). The real value of this constant is between 1350-1370 W/m^2. But we can simplify the number and say that it is 1400 W/m^2 or 1400 J. In other words, this is the energy that every square meter outside the atmosphere, receives from the sun in a perpendicular plane whiting the Earth-Sun line.

If we want to calculate the energy at land level, we have to multiply this number by the surface (in a plane) of the Earth ($\pi \cdot r^2$) and divide it by the surface in a three dimensions sphere ($4\pi \cdot r^2$), using r as the Earth radium. The result is 342 W/m^2 and it is called average solar constant. Only half of the Earth is receiving that radiation because one side is day and the other is night. It also depends on the latitude due to the incident angle of the sun rays.

The radiation coming into the Earth is divided depending on the wave length (λ) in these different categories, from more energetic to less: Ultraviolet (1nm-400nm), Visible Light (400nm-750nm) and Infrared (750nm-1mm). Of course there are so many others but in this work we only need to consider these three.

One big part of the Sun´s energy is absorbed by the atmosphere, approximately 25-60%, depending on the atmospheric conditions, especially in the troposphere.

At the Earth´s surface, the radiation is compound by 49% of infrared, 41% of visible light and 9% by ultraviolet radiation. Of course, it depends on the atmospheric conditions and the vegetation, because clouds absorbs mainly in the ultraviolet region and plants in every region, but mostly in the visible light region of the spectrum (it is used in the photosynthetic process).

On other hand, Earth reflects to space around 30% of the total amount of energy that it receives from sun. It is called albedo effect, and it is caused by clouds, ice and water principally.

So, if Earth receives 342 W/m^2, only 240 W/m^2 (70%) are absorbed, but it is not in a homogeneous way; more is absorbed in the

Equator than in the poles and more by the Earth than by the high atmosphere. It causes the big streams and the heat transport phenomenon which configure Earth climate.

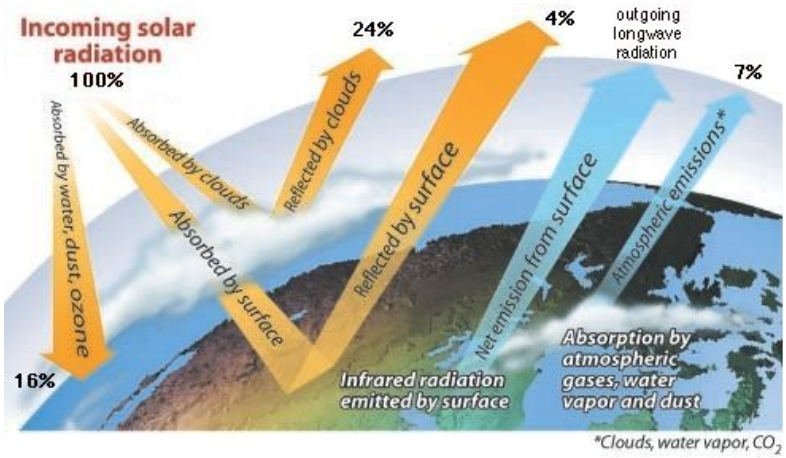

Fig. 1 Percentages of incoming and reflected sun radiation by different Earth elements (www.google.images.com)

The natural greenhouse effect

In physically terms, the kind of radiation that every object emits depends on its temperature (Wien`s radiation law). Based on this law, satellite observations say that the average temperature in the Earth is -18ºC. It corresponds to 240 W/m^2 if we already are in thermic equilibrium. But Earth average temperature is +15ºC which corresponds to 390 Watt/m^2. The 150 W/m^2 difference is caused by the greenhouse effect. The Earth surface emits 390 W/m^2, but 150 W/m^2 are absorbed by the atmosphere, which keeps the temperature above the correspondent temperature. For this reason, satellites can only detect 240 W/m^2 emitted by the high atmosphere.

The 33 Celsius degree difference is caused by the greenhouse effects and it makes possible life on the Earth. In conclusion, the greenhouse effect warms up the atmosphere by capturing the long wave radiation reflected by the Earth.

We have to keep in mind that the energy is always the same. The incoming energy is equal to the outgoing energy because energy can not be created, only transformed. In this case, we are talking about a modification in the wave length. The incoming radiation from the sun is very energetic, it has a very short wave length because the sun is a very hot object. The outgoing energy from the Earth is a long wave radiation which has less energy, but the spectrum is bigger so the total energy is the same.

Greenhouse gases

Curiously, oxygen and nitrogen, which are the principal components of the atmosphere (99%), are totally transparent to the infrared radiation reflected by Earth, so they are totally inert gasses regarding the greenhouse effect (Table 1).

Table 1. The responsible greenhouse gasses (http://en.wikipedia.org/wiki/Greenhouse_gas)

	Relative effect	Real effect
CO_2	1 (reference)	76%
CFCs	15.000	5%
CH_4	25	13%
N_2O	230	6%

The relative effect means that we assign the value 1 to the carbon dioxide activity, and other activities are calculated regarding to this data. As we can see, although chloro-fluoro-carbons have relatively much more effect than carbon dioxide, the big concentration of carbon dioxide compared with CFCs make possible the big effect of CO_2 as greenhouse gas. Carbon dioxide is totally transparent to the incoming radiation from the sun, but it absorbs the reflected infrared radiation by the Earth. That is the reason why it allows the radiation entry in the system, but does not allow it to escape.

The role of the CO2 in the plant physiological processes is also worth to mention. This gas is one of the basic materials of photosynthesis. At constant environmental conditions, the higher the CO2 concentration, the higher the intensity of photosynthesis is. This influence was published among others by *Anda* (2006); *Anda and Kocsis* (2007; 2008).

Clouds have a double effect. By one hand, it is calculated that water vapour can increase the greenhouse effect by 30 W/m^2, absorbing the infrared radiation from the surface. But in the other hand, clouds reflect the incoming radiation from the sun, and it is calculated also that clouds albedo effect is -50 W/m^2. The absolute effect of clouds during the day is a 20 W/m^2 cooling.

It is said that the more carbon dioxide concentration in the atmosphere, the more will be the evaporation and consequently, the cloud formation. We have just said that clouds cause cooling, so here we have one of the polemic points.

Comments on global warming[1]

The main argument of the IPCC focuses on the correlation between the average increase of the temperature of the Earth and the parallel increase in atmosphere CO_2 content. This rise in the CO_2 content is caused by burning fossil fuels, and, what is very important, in the last century. Other human factors influence the atmospheric CO_2 content, as desertification, decrease of rain forests and so on. However, combustion of fossil fuels is by far the most "guilty" of emissions.

Some other natural phenomena may also cause atmospheric alterations in a similar range to the burning of a few GT of oil. Particularly, volcanic activity could shatter the atmospheric balance, apparently so fragile, in a few weeks if the activity is strong. Some examples are the explosion of Krakatoa, the Tungusta meteorite and the eruption of Pinatubo, which caused that kind of changes.

As I mentioned before, IPCC is the political origin of the controversy around global warming. It is also the origin of social and political awareness on this phenomenon (http://www.ipcc-nggip.iges.or.jp/public/gl/lucfspan.html).

1 Personal note: I will use many arguments that say that global warming is a phenomena caused by human activity. Not all of these arguments are totally accepted by the scientific community, but are defended by many others, as well as the IPCC.
However, I also have present in my mind that IPCC is a political organization (it came from the UN, 1989) and is not totally independent of the economics. Furthermore, people who work there are being paid to demonstrate that global warming is caused by human activities; this is the reason for the IPCC´s existence.

In summarize the conclusions of the main IPCC reports are:

- There is an evident climate change
- The cause of this change comes from the large increases in the atmospheric CO_2 with a consequent increase in the greenhouse effect.
- Human activity is responsible for the increase of CO_2 content
- It is necessary to curb emissions
- The models show alarming trends

These assumptions and conclusions are based on mathematical models, which are the origin of the controversy because models can be developed in many ways and even a little change in the same model would predict totally different results.

Let's see what is going on with **temperature and CO_2** depending on the point of view. With respect to temperature, it is necessary to take into account the veracity of the data used for statistical analysis, and not forget the margin of error that these methods carry with them. As an example we could mention the "hockey stick" model (Fig. 2), developed by *Mann et al.* in 1998 (IPCC 2001). It shows temperatures since 1000 AC until nowadays. In the graphic you can see that temperatures decrease slightly between the early 15th century and early 20th century, and then increase dramatically until 1980.

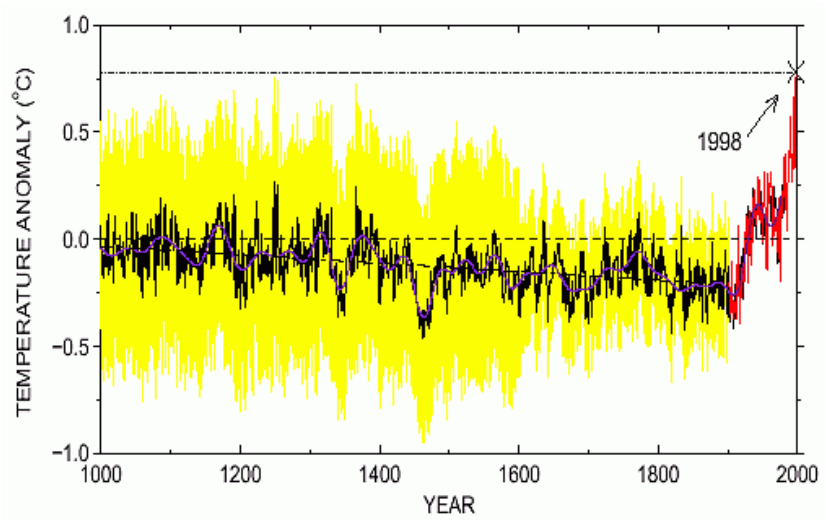

Fig. 2 "Hockey stick" model (IPCC 2001)
http://www.realclimate.org/index.php/archives/2004/12/myths-vs-fact-regarding-the-hockey-stick/

The yellow area is the error margin. In the reconstruction of temperatures before 1850, the margin is so big that they could demonstrate almost whatever they want.

But not only before 1850 we can find some problems with the data. For example, the Fig. 3 shows a statistic register of world temperatures since 1880. This register is compiled by the GISS (Goddard Institute) in the U.S. and the CRU (Climatic Research Unit) of Britain. The graph shows clearly a 0.8 degrees Celsius warming in the period. However, the temperature increase not necessarily corresponds with the actual warming of the atmosphere. The urban character (heat island) of most of the stations among many other reasons induces caution in its interpretation (http://data.giss.nasa.gov/gistemp/).

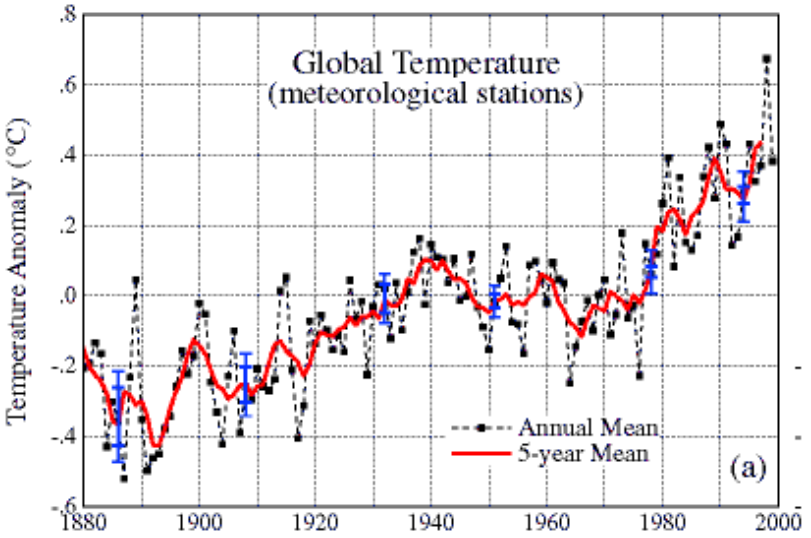

Fig. 3 The global temperature changes from 1880s [GISS from Goddard Institute, USA; CRU Climatic Research Unit from Great Britain (http://data.giss.nasa.gov/gistemp/graphs/)]

Fig. 4 obtained from 48 states in the USA which shows, for a similar period, an evolution of the temperatures that has little or nothing to do with the previous one. Something similar happens with different data register of arctic temperatures. It is very interesting that, coming from different sources and from different world places, both show a big warming between 1920 and 1940, even when the CO_2 levels were lesser than in the present day.

The content of Fig. 5 would be very dramatic since it shows powerful heating in a short time period. But if it were true, the ice melting in the North Pole would be imminent, and large amounts of fresh water would be released, causing some other phenomenon which will be mentioned later (see later **gulf current variations**).

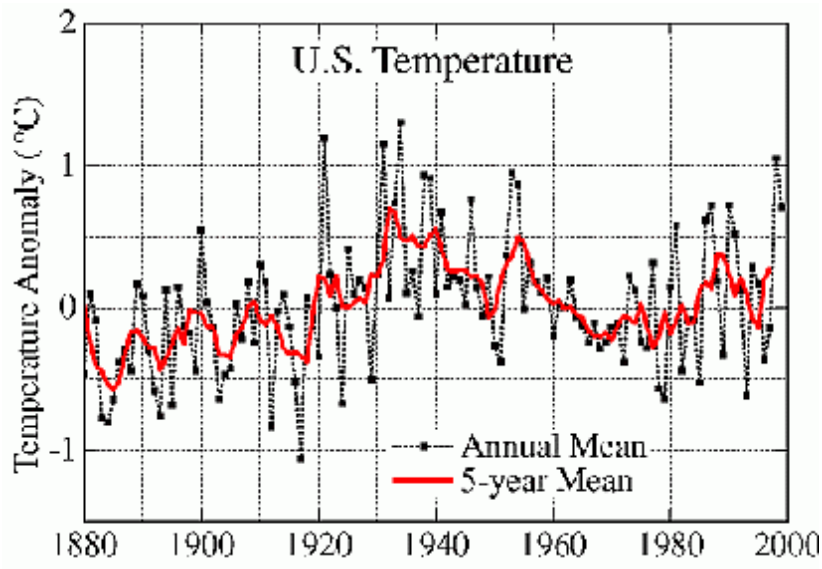

Fig.4 Temperature time series from 1880s [GISS from Goddard Institute, USA; CRU Climatic Research Unit from Great Britain (http://data.giss.nasa.gov/gistemp/graphs/)]

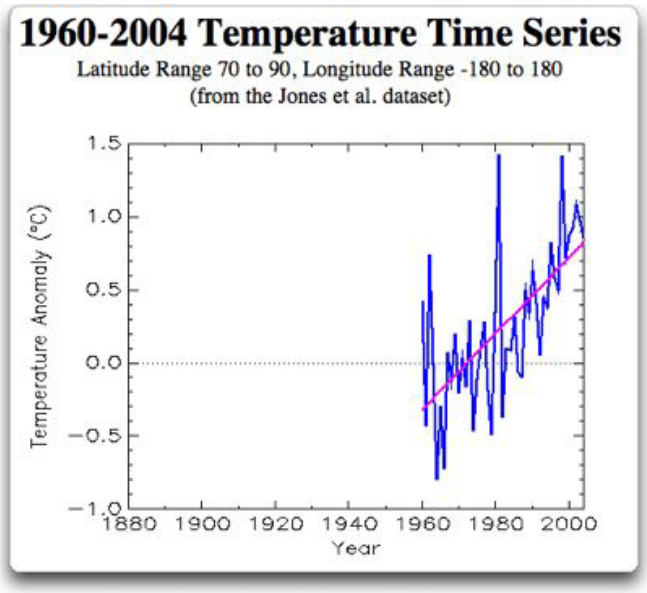

Fig. 5 Short term Arctic temperature increasing (Jones et al. 1994)

But if we use a bigger register, the conclusions may be totally different. In that case, the heating between the twenties and forties was almost the double than nowadays (Fig. 6).

After the "hockey stick" model were publicised in 1998, many scientists who worked for the IPCC became angry and raised their voices to show their disagreement with a study that they considered defective and with no clear procedures. Two of these scientists, *McIntyre and McKitrick* (2005) detailed these errors and defects. Then, they applied the Mann, Bradley and Hughes methodology and they made a new average temperatures index of the Northern Hemisphere for the period 1400-1980, using corrected and updated data.

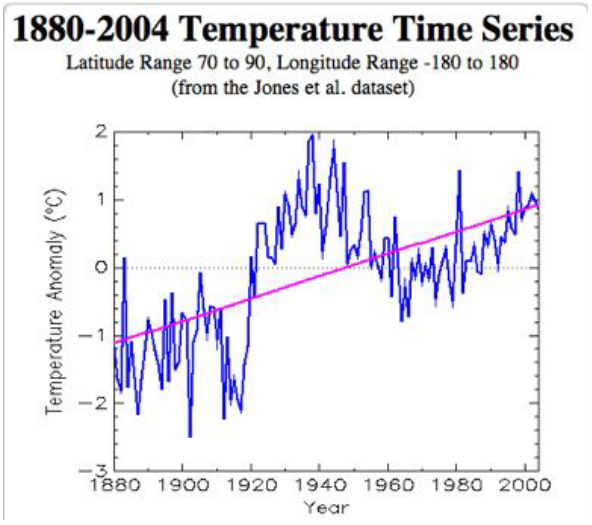

Fig. 6 Long term Arctic temperature change (Jones et al. 1994)

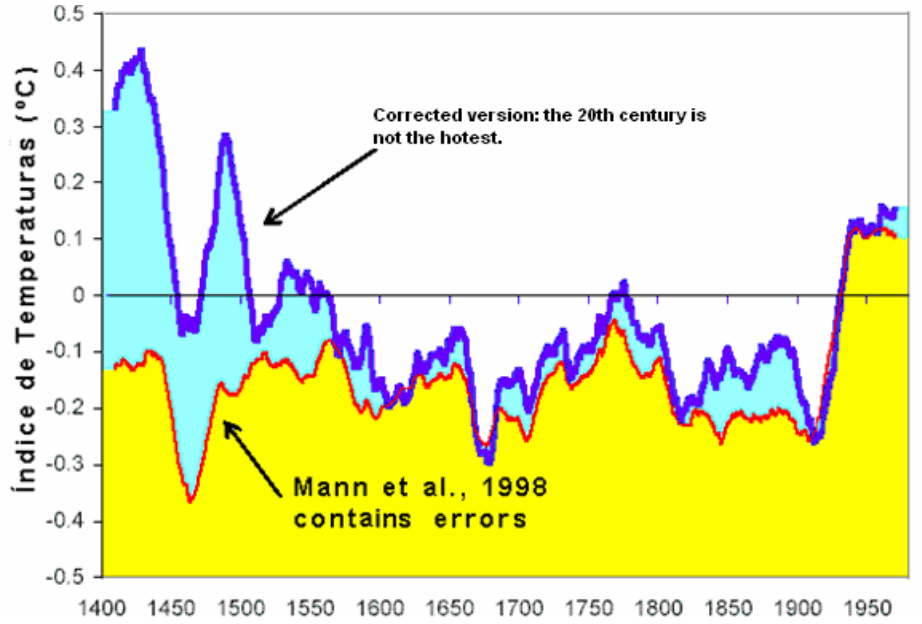

Fig.7 McIntyre-McKitric (2005) *reconstruction of "Hockey Stick"*

The McIntyre-McKitric reconstruction (thick line in Fig 7) shows that the previous climate was warmer than at the end of the 20th century, a conclusion supported by numerous other scientific studies, while the "Hockey Stick" denies this reality.

The world is not in a thermodynamic equilibrium, so that there is not only one single temperature to discuss about it. What we measure in each point is tied to that place through a local thermodynamic equilibrium. A global average temperature does not have a global sense, and that kind of statistic does not state certainly whether the world is warmer or colder than 10, 100 or 1,000 years ago. The temperature only means something at local level, but it can not be

extrapolated to big areas or continents because the thermodynamic conditions vary from point to point.

It is proved that not every point in the Earth is being warmed, there are some places where the glaciers are not suffering ablation and are growing, and some places where the ice layer is increasing. These points are usually in the southern hemisphere. The main heating is being detected in the northern hemisphere.

In order to finish the topics about the temperature, I mention the results of two studies which had been made separately by *Hoyt and Barrett* in 1997 (http://www.warwickhughes.com/hoyt/climate-change.htm). In summary, they say the following:

- The observed heating had been produced mainly in night registers, which is incompatible with a global warming produced by greenhouse effect.

- The observed heating had been detected only in surface, but not in medium and high atmosphere.

- The real observed heating had been detected especially in northern hemisphere and in medium latitudes. The predictions for a greenhouse effect say that it should be detected in the poles more than in any other place.

Something is happening...

Temperature is only one parameter. Temperature evolution is only one indicator of that something may be happening, but there are many others, some quite evident, and others very subtle but not less important.

I cite some examples to illustrate that "something is happening”:

•Decreasing of the polar icecaps

• Decreasing of some glaciers around the globe

• Pure and simple disappearance of some glaciers

• Lowering of the thickness of polar ice cap in the northern hemisphere

• Changes at the Permafrost especially in Alaska and northern Siberia

• Reverse-down of forests Nordic

• Changes in the migration of animals

• Disturbance (advancement) of the flowering of many species in upper and middle latitudes

• Sea level rising (5 cm over the past 100 years)

• Emigration to higher altitudes of species (plants) observed in the Alps

• Zooplancton-decreased in the Atlantic due to lack of nutrients, caused by the temperature increasing in some sea areas

• Alterations in the stream of “El Niño”

• Alterations in the insect’s population of high latitude forest areas

• Emergence of foreign larvae and insects in certain areas

All these symptoms clearly indicate that something is happening. Otherwise very different causes produce these phenomena.

As we mentioned before, greenhouse effect increasing is produced by the growing accumulation in the atmosphere of gases capable of absorbing energy radiated by the Earth in the infrared range. Despite the most important greenhouse gas being water vapour its variation is considered as result of the variations in CO_2 concentration in the atmosphere.

The effect of other greenhouse gases, mainly CH_4, CFCs and O_3, N_2O is always expressed in the equivalent amount of CO_2 by effect.

On one hand, it is known that carbon dioxide is responsible for 22% of the greenhouse effect, and it is the mainly one. On the other hand, human activity, particularly fossil fuels burning, is responsible for the emission of very substantial quantities of this gas.

It is not easy to establish the direct relation? In fact, it seems easy, but it is not. Let's see Table 2!

The increase in the atmospheric CO_2 concentration stands at around 1.4 ppmv/year. This increase does not seem parallel to the increasing in combustion of coal and petroleum, which has risen from 4.4 GT in 1972 to 8 GT in 2000.

The models and projections derived from the IPCC assume virtually that CO_2 accumulates in the atmosphere. Based on this premise, the global warming predictions leading to highly catastrophic conclusions where temperature would increase to the order of 2-3 ºC.

But the CO_2 cycle in the atmosphere is far from being known with accuracy, and contrary to the IPCC assumptions put at 200 years, recent studies seem to show that this cycle is 35/40 years.

Table 2. Emission values, thermo anomalies, CO_2 concentration and carbon dioxide by ice-thermometer (www.google.com)

	Emissions rate	Satellite temperature anomaly	Surface temperature anomaly	Surface temperature, trend removed	CO2 concentration	Increase of CO2	CDT reading
	Pg/year	°C	°C	°C	ppmv	ppmv	ppmv
1979	5.35	-0.026	-0.15	0.03	339.68	1.34	-0.23
1980	5.28	0.122	-0.11	0.05	338.52	1.84	0.27
1981	5.11	0.079	-0.07	0.07	339.76	1.24	-0.33
1982	5.07	-0.127	-0.16	-0.04	340.76	1.20	-0.37
1983	5.06	0.059	0.03	0.13	342.61	1.65	0.08
1984	5.23	-0.236	-0.19	-0.11	344.25	1.64	0.07
1985	5.40	-0.175	-0.21	-0.14	345.73	1.48	-0.09
1986	5.59	-0.105	-0.12	-0.07	346.97	1.24	-0.33
1987	5.72	0.130	0.02	0.05	348.75	1.78	0.21
1988	5.94	0.130	0.04	0.05	351.31	2.56	0.99
1989	6.05	-0.091	-0.03	-0.04	352.75	1.44	-0.13
1990	6.10	0.090	0.14	0.11	354.04	1.29	-0.28
1991	6.18	0.119	0.08	0.03	355.48	1.44	-0.13
1992	6.10	-0.227	-0.06	-0.13	356.29	0.81	-0.76
1993	6.07	-0.201	-0.02	-0.11	356.99	0.70	-0.87
1994	6.22	-0.073	0.05	-0.05	358.88	1.89	0.32
1995	6.41	0.085	0.18	0.06	360.91	2.03	0.46
1996	6.52	-0.021	0.01	-0.13	362.69	1.78	0.21
1997	6.29	0.002	0.22	0.06	363.82	1.13	-0.44
1998	6.32	0.462	0.36	0.18	366.70	2.88	1.31

Moreover, the CO_2 content in the oceans is 50 times higher than in the atmosphere and we far from know the CO_2 absorption capacity by the oceans, at least quantitatively.

The controversy is served again

An example: the Gulf Stream

The description and development of the heat transfer belt widely escapes from the scope of this work. However the overall conclusions are the following:

Sea streams play an extraordinary role in the heat distribution in the Earth. They are responsible for the latitudinal heat distribution, carrying the heat excess from Equator to northern latitudes, warming those areas (*Broecker* 1987, *Broecker and Kunzig* 2008).

There are two different kinds of streams (Fig. 8):

- Hot streams, which come from Equator to northern latitudes, moving through the ocean surface.

- Cold streams, which come from poles to Equator, carrying a lot of nutrients which can feed the living organisms and fish.

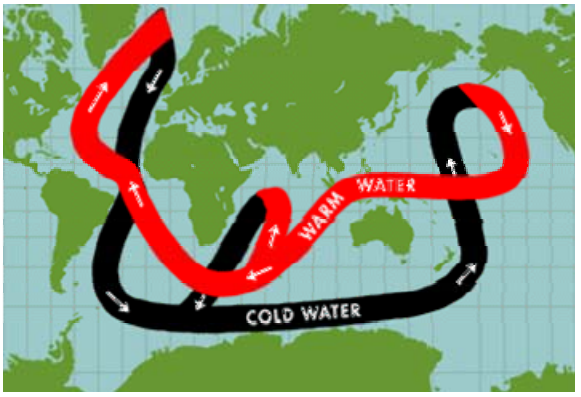

Fig 8. The main global streams (The Broecker conveyor belt after the original publication of Broecker from 1987)

The responsible engine for this movement is called thermohaline circulation. It is due to the differences in the density caused by the different salt concentrations and differences in the

temperatures. The more salty the water, the heavier it is, and the more cold the water, the more dense it is also.

During the winter, a lot of water is frozen, and during this transformation, a lot of salt is released from the water before it becomes ice. This very cold and salty water is quickly moving down and it displaces close to the ocean floor, direction to Equator. During this travel, that water masses pick up a lot of nutrients and cooler the continents where it passes throw.

During the approximation to Equator, it water is warmed and helped by some other factors, as winds, big amounts of very nutrients-rich water comes up, causing oceanic blooms and very good for fishery (for example, in front of Peru's coast).

In the other way, big amounts of poor-nutrient water from Equator are moving by the surface to the North and South Poles. This stream warms a lot of places which, due to the geographic situation, there should be much colder than really are, as British Islands.

But if the North Pole is melting, a lot of fresh water will be released and the water will not be able to move down, so the stream will stop. If it happens, many places in some northern regions will be much colder than now and the Equator heat will not be distributed in the Earth. It is said that if it happens, another ice age would start (*Broecker and Kunzig* 2008). So here, we have other point which is still not clear.

Conclusions – other new questions and concerns

The aim of this work was double: First described in a clear and simply way the greenhouse effect, and another put on the table data and evidence from different sources to enable the reader have an idea, may be quite superficial, about the controversy arisen the concept global warming, the complexity of the phenomenon and the interaction among its possible causes. I hope I have fulfilled both goals.

I believe that the climate analysis with statistical methods is not very accurate because it depends on many variables very volatile and interlinked with one another. Besides the studies being carried out does not take into account the geological scale of the Earth's climate, which has changed on numerous occasions, both naturally and without that the man was also acting negatively. An example would be during the Mesozoic Era (225-65 million years ago) when the mean temperature of the Earth was about 5ºC higher than the current one.

If the temperature rise was true, we should have the following question: were we the cause or the only cause? Why are not considered other natural factors as solar cycles and astronomical causes? In Earth's history there have been numerous increases and decreases in the concentration of CO_2 in times in which they did not know the meaning of the "industrial revolution" and even less were used "fossil fuel" as at present, and we still don't know the real causes of these fluctuations. In my opinion, something is happened, but we still don't know exactly what, and of course, we can not be sure if we are the responsible.

Acknowledgements

I'm grateful to my teacher, Angela Anda for her assistant to publish this study.

References

Anda, A. 2006. Modeling maize response to climate modification in Hungary. *(CBCS)Commun. Biometry Crop Sci.* 1. 2: 90-98. http://agrobiol.sggw.waw.pl./cbcs)

Anda, A. and Kocsis, T. 2007. Evaluation of climatic changes on maize energy consumption in Hungary. GSB. *The Eur. J. of Plant Sci. and Biotechnol.* Vol.1. 2: 200-205.

Anda, A. and Kocsis, T. 2008. Impact of atmospheric CO2 enrichment on some elements of microclimate and physiology of locally rown maize. *Applied Ecology and Environmental Research* 6. 1: 85-94. www.ecology.uni-corvinus.hu

Broecker, W. S. 1987. Unpleasant suprises in the greenhouse? *Nature,* 328: 123-126.

Broecker, W. S. and R. Kunzig 2008. Fixing Climate: What Past limate Changes Reveal About the Current Threat--and How to Counter It. Hill and Wang Publ. US/Profile Books, UK.

IPCC 2001. Third Assessment Report, Climate Change. http://www.google.com/search?hl=en&q=ipcc+2001+third+assess ment+re port&aq=1&oq=IPCC+2001

IPCC 2007. http://www.ipcc-nggip.iges.or.jp/public/gl/lucfspan.html

Jones, H.G., Davies, T.D., Ohmura, A. and Morris, E.M., 1994. Snow and Ice Covers; Interactions with the Atmosphere and Ecosystems. *International Association of Hydrological Sciences,* Publ. No. 223, Wallingford, U.K. 340pp.

McIntyre, S. and McKitrick, R. 2005. Hockey sticks, principal components and spurious significance. *Geophysical Res. Letters*, Vol. 32, LXXXXX, doi:10.1029/2004GL021750.

http://www.giss.nasa.gov/research/paleo/pliocene/page3.html

http://www.warwickhughes.com/hoyt/climate-change.htm

http://en.wikipedia.org/wiki/Greenhouse_gas

http://data.giss.nasa.gov/gistemp/graphs/

NEW APPLIED TECHNIQUES IN EVALUATION OF HYPERSPECTRAL DATA

Veronika Kozma-Bognár [1], *kbv@ex1.georgikon.hu*
József Berke [2], *berke@gdf.hu*

1-University of Pannonia, Georgikon Faculty, Keszthely
2-Dennis Gabor Applied University, Basic and Technical Sciences Institute, Budapest

Abstract

Multiband aerial imagery in remote sensing is a technology used more and more widely in present days. It can excellently be used in research fields where there is need for high spectral resolution images in order to obtain adequate level results. At present, data collection is of a much higher level than processing and use. As the technical development of sensors is followed by a significant delay in data processing methods and applications, it seems reasonable to refine processing methods as well as to widen practical uses (agriculture, environmental protection).

The quantity and complexity of the data supplied by multispectral and hyperspectral sensors are extremely high, so in order to analyse them, an adequate level of hardware and software infrastructure is needed. The circle of supporting programs is quite limited. In the case of several GIS software (ENVI, IMAGINE), independent digital image processing modules include the main image processing methods (maximum likelihood, cluster analysis etc) applicable for multi-channel images.

In the year of 2004, a new examination method based on fractal structure (Berke 2004) was introduced, which, according to our experiences, has made more accurate spectral measurement possible as opposed to other techniques. The mathematical process named spectral fractal dimension (SFD) is directly applicable in multi-dimension colour space as well, making thus possible to choose new examination methods of multiband images. With the help of SFD, it is possible to obtain more useful data offered by high spectral resolution, or to choose the bands wished to process applying different methods later.
In the present publication, the mathematical basis of the SFD parameter will be described as well as some possibilities for its practical use (spectral curves, examination of noisy images). The practical applicability of SFD-based spectra in the case of important plant cultures will be introduced, and SFD-based spectrum directories will be suggested to set up. A new, SFD-based calculation method will be suggested for red edge inflection point.

Keywords: Hyperspectral Remote Sensing, Image Processing, Multispectral Remote Sensing, Spectral Fractal Dimension, Red Edge Inflection Point, Stress Detection, Spectral Noise Detection

Összefoglalás

Napjainkban a távérzékelési módszerek közül a többsávos légifelvételezés egyre szélesebb körben használt technológia. Kiválóan alkalmazzák olyan kutatási területeken, ahol a megfelelő szintű eredmény elérése érdekében nagy spektrális felbontású felvételekre van

szükség. Jelenleg az adatok gyűjtése fejlettebb szinten áll, mint azok feldolgozása, hasznosítása. Mivel az érzékelők technikai fejlődését a feldolgozási módszerek és az alkalmazások jelentős késése követi, indokolttá válik a feldolgozási eljárások pontosítása valamint a gyakorlati alkalmazások (mezőgazdaság, környezetvédelem) lehetőségeinek kibővítése.

A multi- és hiperspektrális érzékelők által szolgáltatott adatok mennyisége, és komplexitása rendkívül nagy, ezért elemzésükhöz megfelelő szintű hardver és szoftver eszközháttérrel kell rendelkezni. A feldolgozást támogató programok köre elég korlátozott. Számos térinformatikai szoftver esetében (pl. ENVI, IMAGINE) önálló képfeldolgozó modulok tartalmazzák a sok csatornaszámú felvételek esetében alkalmazható főbb képfeldolgozási módszereket (maximum likelihood, cluster analysis, stb.).

A 2004. évben bevezetésre került egy olyan új - fraktálszerkezetre épülő - vizsgálati módszer (Berke, 2004), amely tapasztalataink alapján más technikákhoz képest spektrálisan pontosabb mérést tesz lehetővé. A spektrális fraktáldimenzióként (SFD) elnevezett matematikai eljárás közvetlen alkalmazható több dimenziós szintérben is, lehetővé téve ezzel a többsávos felvételek vizsgálati módszerének újszerű megválasztását. Segítségével növelhetjük a nagy spektrális felbontás kínálta hasznos információk kinyerését vagy olyan sávok kiválasztását, amelyeket más módszerekkel kívánunk feldolgozni.

Jelen publikációban bemutatásra kerül az SFD paraméter matematikai alapjai mellett a gyakorlatban történő alkalmazás néhány lehetősége (spektrumgörbék, zajos képek vizsgálata). Bemutatjuk az

SFD alapú spektrumok gyakorlati alkalmazhatóságát fontosabb növénykultúrák esetén, valamint javasoljuk SFD alapú spektrumkönyvtárak létrehozását. A vörös-él számítás új, SFD alapú számítási módszerére teszünk javaslatot.

Introduction

Remote sensing images can be classified according to several points, eg. the aim of data collection, the height of where the image was taken, spatial resolution, wave length range, or the number of channels. Based on the number of channels, the following classes can be identified:

- Panchromatic images: 1 channel
- Colour images (RGB cameras): 3 channels
- Multispectral images: 4-20 channels
- Hyperspectral images: 21- channels (EU Council, 2003)

Panchromatic images are usually of high spatial resolution, and are made integrating visible and near infrared range. Multispectral images contain several channels of wider band channels, whereas hyperspectral images are of narrow band width (0,01 μm) with greater number of channels (Sabins, 1987; Schowengerdt, 2007). In images taken in more than one channels-due to high spectral resolution-, landmarks and surface details can more easily be identified than using only one channel. That is the reason why the application of multispectral and hyperspectral imagery devices is getting more and more emphasis nowadays.

Remote sensing applies and records electromagnetic energy reflected or emitted by the objects on the soil surface. Detecting devices primarily detect reflected energy with wavelengths under 3000 nm, whereas with wavelengths over 5000 nm, emitted energy is detected. Elements of different characteristics will take a different reflection (or emission) value in certain wavelength ranges, depending on the physical and electromagnetic features, as well as the wavelength of the electromagnetic radiation of a given substance. The curve of reflection values of objects represented in a wavelength graph is called a spectral reflection curve (Sabins, 1987; Berke et al., 2004). Based on this curve, microorganisms, minerals, plants, buildings and artificial materials can easily be identified, as different materials have different reflection curves due to their different characteristics. Digital spectral libraries (USGS Digital Spectral Library, Aster Spectral Library), containing 'spectral fingerprints' recorded under given conditions and collected in libraries, play a significant role in spectral identification. The standard spectral profiles are usually used as references in the identification of elements.

In the scientific literature on surface reflectance, several indexes can be found that are generated from the reflection curve values and certain differences. NDVI (Normalised Difference Vegetation Index) is a vegetation index that is a first generation index widely spread in remote sensing showing photosynthetically active vegetation. In case the examined plant file contains soil spots as well, then SAVI (Soil-Adjusted Vegetation Index) is to be used. Red Edge Index is considered to be a second generation - or, after Broge and Mortensen (2002), a

new generation - index, which describes the shape and relative situation of the reflection curve (Red Edge Inflection Point - REIP). Throughout the evaluation of the curve, the health state, stress toleration ability, chlorophyll content, and infection level of plants etc. can be judged from the shift of the inflection point (Varshney and Arora, 2004; Jung, 2005; Tamás and Róth, 2008). Out of several, two relatively simple calculation methods have been used in practice:

Calculating REIP according to Clevers et al., (2002):

$$\lambda_{re} = 700 + (740-700)\,[(R_{re} - R_{700})/(R_{740} - R_{700})], \text{ ahol } R_{re} = (R_{670}+R_{780})/2 \quad \textbf{(1)}$$

Calculating REIP according to Mutanga és Skidmore (2004):

$$\lambda_{re} = 695 + (742-695)\,[(R_{re} - R_{695})/(R_{742}-R_{695})], \text{ ahol } R_{re} = (R_{663}+R_{788})/2 \quad \textbf{(2)}$$

where R_{re} = reflectance of inflection point,

R_λ = reflectance at λ wavelength.

In multi-band imagery technologies, data are recorded in the form of a ’data square’, each band of which is an image of the examined area. The intensity values read from the vertical values of image elements of the same area give the steady distribution spectrum of the surface material of the area. The data recorded by multispectral and hyperspectral sensors are raw figures that can be turned into reflectance values having acquisited spectroradiometric references later on the spot and other corrections (eg. atmospheric). Reflectance data gained this way take into account the continuously measured reflectance of incoming sunshine as well. After this correction, the recorded spectrum of the image is suitable for comparison to other eg.

laboratory spectra (Hargitai, 2006). In digital spectrum libraries, data defined under laboratory circumstances are collected, in which no effects of natural phenomena are included. They usually include the data of pure or mixed materials, whereas our remote sensing devices integrate a lot of other unique information in their output data depending on the sensor and atmospheric characteristics, which can significantly differ from one another. In order to acquire more accurate reference data, often on-the-spot spectrometers are used with the use of which differences between sensors can partly be compensated (applying the same series of sensors), though the atmospheric effect can not. A further problem is that the accuracy of on-the spot spectroscopic examinations is also influenced by several factors (eg. calibration, viewing angle, type of sensor, weather conditions), which can not be post-corrected or repeated (Burai, 2007).

Materials and Methods

The location of our examinations was 15 km from Keszthely, Hungary, a test area near Várvölgy, Hungary, where there are several agricultural fields. We have been taking multispectral and hyperspectral aerial images of the scene since 2006. The first hyperspectral images were taken in 2007, using an AISA Dual hyperspectral sensor, which is one of the most significant systems of the European Union (Nagy et al., 2008). AISA Dual, as member of the AISA camera series developed by SPECIM, Finland, was set up by joining AISA Eagle and AISA Hawk sensors in a dual carrier. The two sensors are capable of collecting data synchronically of the same earth band in the 400-2450 nm spectral

range, in maximum 498 bands. Most important features of the sensors can be seen in Table 1. (based on Burai, 2006).

Table 1. Technical parameters of AISA Dual

	VNIR sensor (Eagle)	**SWIR sensor (Hawk)**	**AISA Dual**
Spectral range	400-970 nm	970-2450 nm	400-2450 nm
Spectral channels	244	254	498
Spectral band width	2.3 nm	5.8 nm	
Spectral depth (bit)	12	14	14
Spatial pixel number	1024	320	320
Optics	18.5 mm	22.5 (or 14) mm	18.04
Image creation speed	Up to 100 image/s	Up to 100 image/s	Up to 100 image/s

In the region of Keszthely, Hungary, there have been flights two times. On 21. May 2007, after the test area of Várvölgy, the Valley of the River Zala and several parts of the Little Balaton were captured. On 19. June 2007, the Várvölgy area was monitored. The sensor acquired data from a height of nearly 1200 m. The result was images of 1m/pixel resolution in 359 spectral bands (Kozma-Bognár et al., 2007). Owing to high channel number, several bands were found that contained different

kinds of noise. Based on visual interpretation, three different noise types were identified (Kozma-Bognár, 2008):

- Geometric,
- Sensor-caused,
- Atmospheric.

Figure 1 shows an AISA image with no noise (254 bands), whereas Figure 2 shows a band with atmospheric noise (273 bands) after geometric and radiometric corrections carried out with the help of a special software named Caligeo (Specim Spectral Imaging Ltd.).

In the noiseless images taken on 19. 06. 2007, land usage, agricultural methods can well be identified, borders of fields and agricultural directions can well be distinguished. Detailed information is obtained on the spectral features of the surface, although the resolution does not achieve sub-meter accuracy.

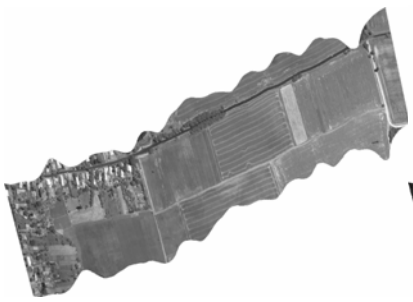

Figure 1. Noiseless AISA image of Várvölgy - image of Várvölgy 254th band

Figure 2. Noisy AISA image of Várvölgy - 273rd band

Adequate results can also be achieved if we need high terrain resolution but not several channels, or in the lack of financial background to use this equipment, with the application of handheld

cameras attached to an aeroplane. Multispectral images were taken of the Várvölgy test area which achieved sub-meter terrain resolution (10-30 cm). Applied digital devices: Canon EOS digital camera for visible light range (400-700nm), Canon EOS digital camera for near infrared range (720-1150 nm), and a thermal infrared (12 000 nm) camera developed by Hexium Company (Hexium Műszaki Fejlesztő Kft.). The images taken by the cameras were georeferated, thus they became suitable for adequately exact measurements as well as analysis (Fig 3.) (Berke and Kozma-Bognár, 2008).

Terrain reference data were acquisited at the time of the flight or shortly afterwards. Our primary aim was to map the plant cultures of the area, and we identified several types of vegetation. During later flights, changes were also recorded. The following material and data were collected:

- GPS data (Busznyák et al., 2008),
- Meteorological data,
- Colour temperature data,
- Sample soil data.

The obtained data were recorded in a protocol each time, and the images taken by handheld cameras throughout our work were also enclosed (Kozma-Bognár et al., 2008).

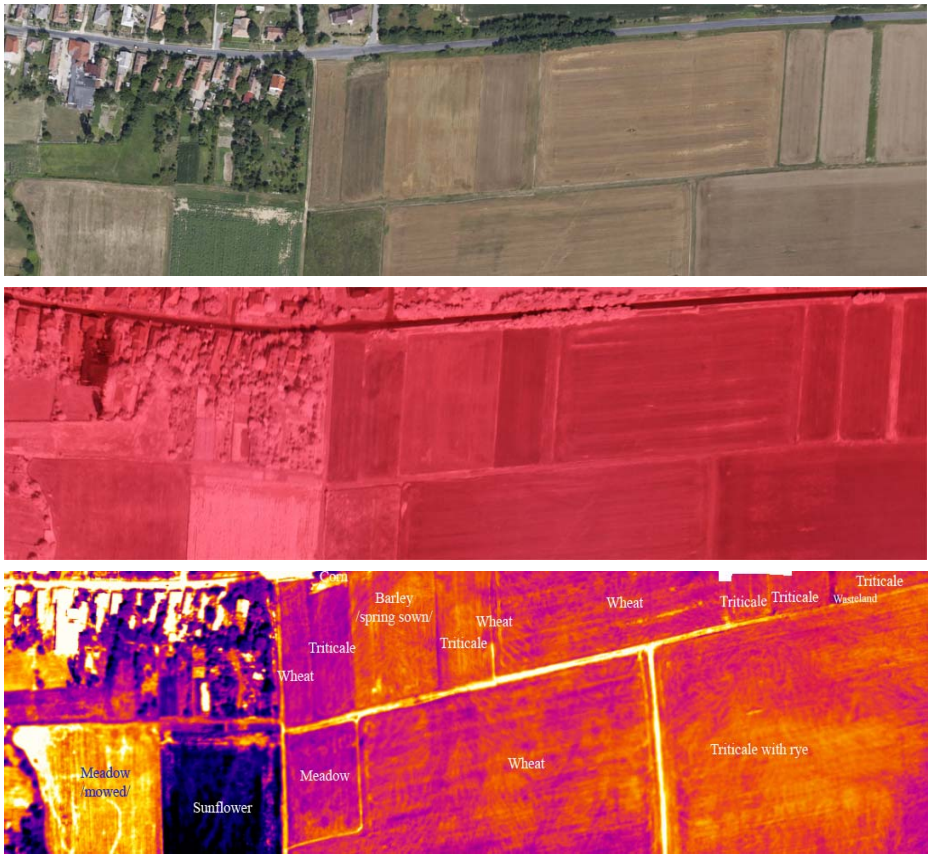

Figure 3. Matched and georeferenced aerial images in the visible (A), near (B) and far infrared (C) range, respectively, of the Várvölgy test area in Zala County, Hungary (photos taken on 19 June, 2007).

When starting the spectral fractal dimension measurement of the different vegetations, we started off the multispectral and hyperspectral images of Várvölgy and their characteristic reference data. SFD (SFD official website) is a structure examining process derived from general fractal dimension (Mandelbrot, 1983; Peitgen and Saupe, 1988). Not only is it suitable for measuring spatial structures, but also for measuring the colour structure of spectral bands, and it also gives

enough information on the (fractal) features of colours and shades (Berke, 2004; Berke, 2006; Berke, 2007; Berke 2008).

Let spectral fractal dimension (SFD) be:

$$SFD = \frac{\log \frac{L_{S2}}{L_{S1}}}{\log \frac{S_{S1}}{S_{S2}}} \quad \textbf{(3)}$$

where L_{S1} and L_{S2} are measured spectral length on N-dimension colour space, S_{S1} and S_{S2} are spectral metrics (spectral resolution of the image).

In practice, N={1, 3, 4, 6, 8, 10, 12, 32, 60, 79, 126, 224, 242, 254, 488, 498, …}:

- N=1 black and white or greyscale image
- N=3 RGB, YCC, HSB, IHS colour space image
- N=4 traditional colour printer CMYK space image, some CMOS sensor
- N=6 photo printer CC_pMM_pYK space image, Landsat ETM satellite images
- N=32 DAIS7915 VIS_NIR or DAIS7915 SWIP-2 sensors
- N=60 COIS VNIR sensor
- N=79 DAIS7915 all
- N=126 HyMap sensor
- N=254 AISA Hawk sensor
- N=488 AISA Eagle sensor
- N=498 AISA Dual sensor.

In practice the measure of spectral resolution can be equalled with the information theory concept of $\{S_i=1, \ldots, S_i=16$, where i=1 or i=2$\}$ bits. Typical spectral resolution:

- Threshold image -1 bit
- Greyscale image - 2-16 bits
- Colour image - 8-16 bits/bands.

On this basis, spectral computing is as follows:

i. Identify which colour space the digital image is
ii. Establish spectral histogram in the above space
iii. Half the image as spectral axis
iv. Examine valuable pixels in the given N-dimension space part (N-dimension spectral box)
v. Save the number of the spectral boxes that contain valuable pixels
vi. Repeat steps iii-v until one (the shortest) spectral side is only one (bit).

In order to compute dimension (more than two image layers or bands and equal to spectral resolution), the definition of spectral fractal dimension can be applied to the measured data like a function (number of valuable spectral boxes in proportion to the whole number of boxes), computing with simple mathematical average as follows:

$$SFD_{measured} = \frac{n \times \sum_{j=1}^{S-1} \frac{\log(BM_j)}{\log(BT_j)}}{S-1} \qquad \textbf{(4)}$$

where

- n – number of image layers or bands
- S - spectral resolution of the layer, in bits – see Eq. (4.2)
- BM_j - number of spectral boxes containing valuable pixels in case of j-bits
- BT_j - total number of possible spectral boxes in case of j-bits

The number of possible spectral boxes (BT_j) in case of j-bits as follows:

$$BT_j = (2^S)^n \quad \textbf{(5)}$$

Results

10 parts of field were examined, where 5 different kinds of vegetation could be distinguished: corn, triticosecale, wheat, sunflower and uncultivated land. The examinations included other objects as well, like the road, and the wood band along it which mainly consisted of wattle. Measuring the above introduced SFD structure parameter band by band we were the first to make wavelength-based 16-bit spectral curves 'fingerprints' (Kozma-Bognár et al., 2008) of these plants and objects (Fig. 4) as well as of the whole images for noise analysis (Fig. 5).

Based on Figure 4 (and the acquired data), plant cultures can definitely be distinguished, and the most adequate spectral bands for certain examinations can be identified. In Figure 5, the curves of the average of the wood, the road and the above mentioned cultivated

plants can be seen depending on the number of channels. The above statements can clearly be seen on it.

Analysing the features of the curves made of the whole bands, noisy bands can directly be suspected.

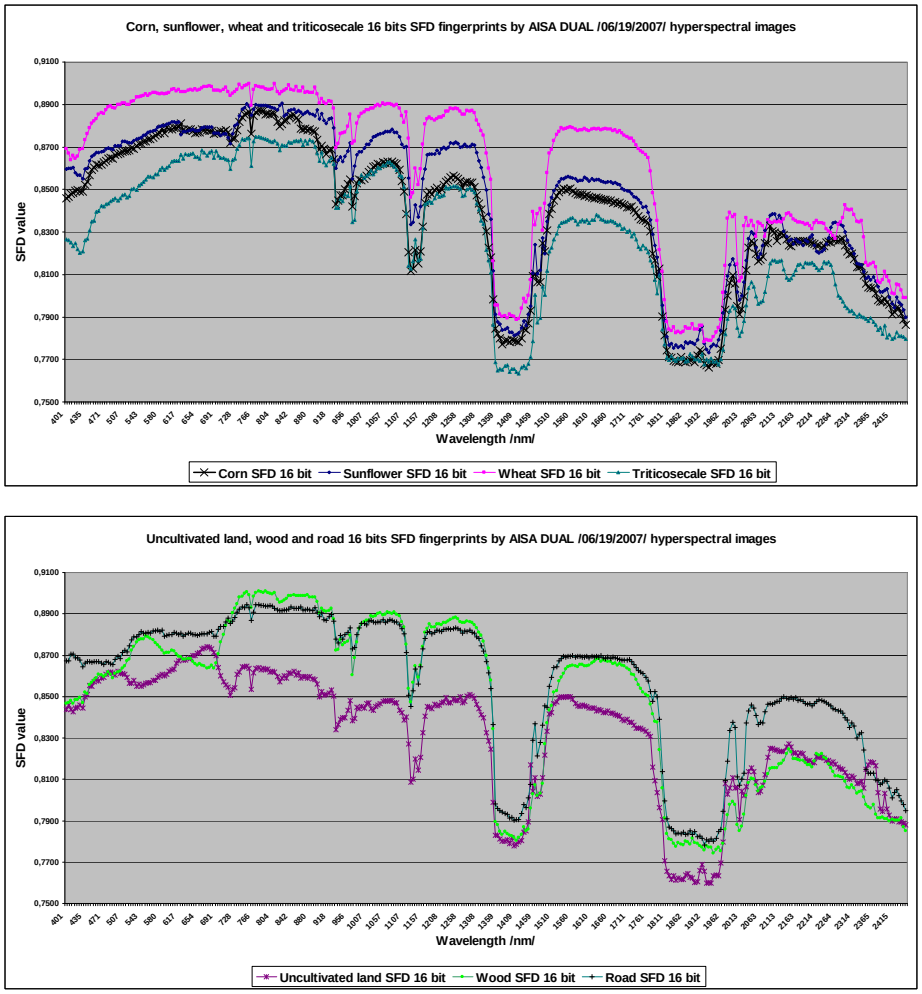

Figure 4. Spectral 16-bit SFD 'fingerprints' of corn, sunflower, wheat, and triticosecale (above picture) and of uncultivated land, wood and road (bottom picture) based on AISA Dual data

It was understood that the noise on the whole image (e.g. atmospheric effect) makes colour structure significantly worse, that is, the SFD values significantly and quickly decrease, maybe oscillate. Such ranges are bands are 116-125, 146-154, 183-204, 284-359. All this can clearly be seen in the images in Fig. 1 and 2, where SFD_{2fig}= 0,4451, SFD_{1fig}=0,1622. The given ranges are the same as the noisy ranges identified by visual interpretation.

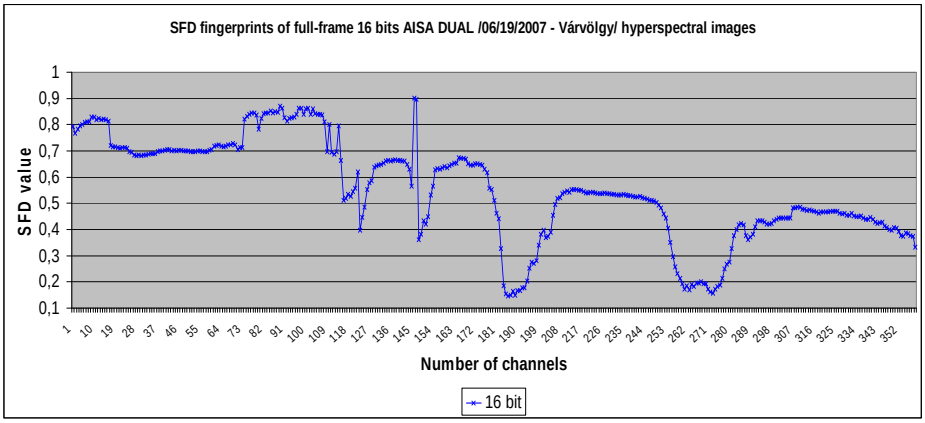

Figure 5. 16-bit spectral SFD fingerprint of the whole AISA Dual image (19. June 2007, Várvölgy) for the identification of noisy bands

In order to identify the inflection point of the red edge in an experimental way, comparing analysis was carried out. For this analysis, the relations suggested by Clevers et al., (2002) and Mutanga and Skidmore (2004), their SFD and reflectance based calculation connections (Fig 6) (1), (2) were used.

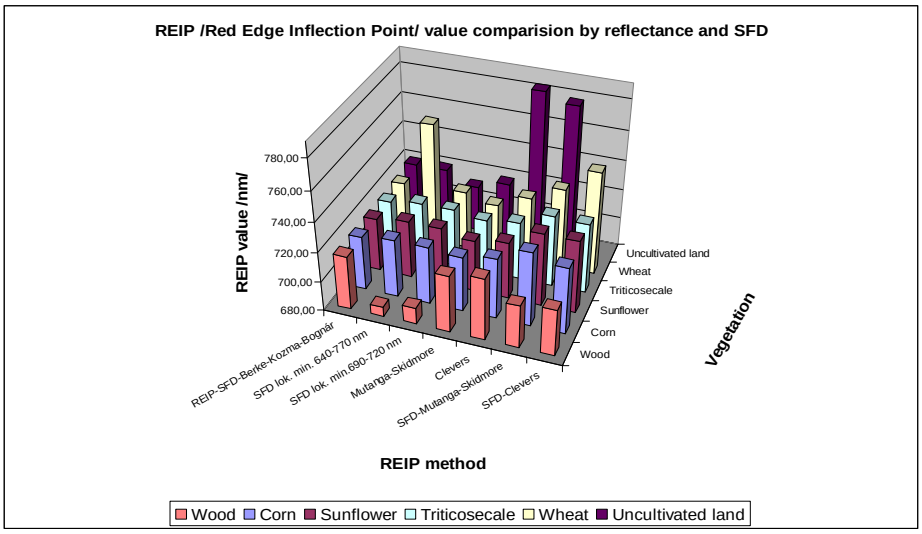

Figure 6. Red Edge Inflection Point identification on AISA Dual images using SFD fingerprints and reflectance data

Based on our AISA Dual images we can state that in the case of plant vegetation, in the 640-770 nm and 690-720 nm ranges on SFD based spectra 'fingerprints', red edge inflection point can directly be identified by searching a local minimum (Fig 7).

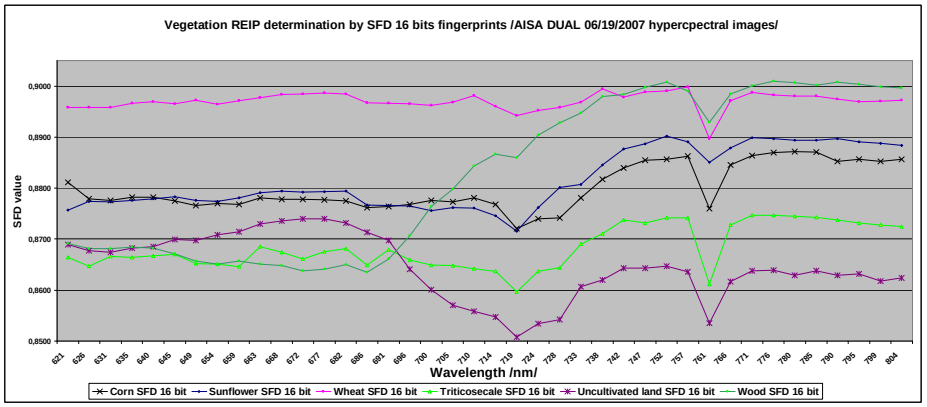

Figure 7. Identification of red edge inflection point on 16-bit SFD curves of AISA Dual images based on local minimums

It is therefore suggested that on SFD curves, red edge inflection point be according to the following connection (Table 2.):

$$\lambda_{re} = 690 + \{SFD_{AVERAGE}\ (690\text{-}720)\}*30 \quad \textbf{(6)}$$

Table 2. Measured and calculated data for red edge inflection point identification in nanometer, based on 16-bit SFD curves and reflectance data of AISA Dual images

	REIP-SFD-Berke-Kozma-Bognár	SFD lok.min. 640-770 nm	SFD lok.min. 690-720 nm	Mutanga - Skidmore	Clevers	SFD-Mutanga - Skidmore	SFD-Clevers
Corn	716,29	719,07	719,07	717,19	720,89	730,31	725,11
Sunflower	716,26	719,07	719,07	714,80	718,49	729,43	729,42
Wheat	716,89	761,28	719,07	714,41	723,78	733,87	749,65
Triticosecale	715,93	719,07	719,07	716,18	718,98	728,20	727,50
Uncultivated land	715,75	719,07	719,07	711,10	717,36	783,23	777,74
Wood	716,36	686,44	691,09	718,51	721,88	709,05	711,52

Based on measurements on the images taken with visible, infra and thermo cameras it can be stated that, in the case of plant vegetation, in the 660-820 nm range, on SFD based spectra 'fingerprints', the local minimum is (Fig 8.) 780 nm. All this can be derived mainly from the different type sensors and multispectral data. This means that, though the SFD based measurements we described make different terrain and spectral resolution image data procession possible, the correspondence we suggested under (6) is useable with SFD values measured in hyperspectral data, but not in multispectral ones.

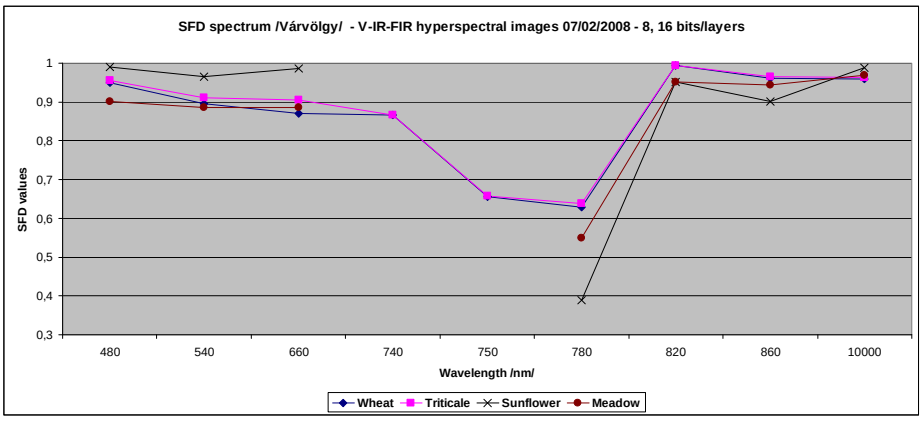

Figure 8. Identifying red edge inflection point based on SFD curves of multispectral images of visible, infra and thermo cameras

Conclusion

The SFD-based data processing method we have developed is directly built on calculations on the structure of image data from remote sensing devices (Berke, 2006), does not necessarily require the application of complementary aerial or terrain radiation sensors, still it gives well-applicable information in several cases. SFD-based structure data are less sensitive to terrain, atmospheric or other correction factors, as they are based on logarithmic calculations. Fingerprints have been developed that, besides terrain identification, can also be calculated using only image information, thus avoiding disadvantages deriving from the lack or inaccuracy of the above mentioned corrections. SFD spectral curves have been created, with the help of which given surface shapes can be described, characterised, identified and mapped similarly to reflectance curves. When creating a REIP index, SFD spectral curve might even give an easier calculation result.

For the identification of red edge inflection point, an experimental correspondence is suggested (6), which, similarly to the presently used experimental correspondence, gives an easily calculable result with the use of SFD spectral curves.

References

Aster Spectral Library: http://speclib.jpl.nasa.gov/ .

Berke, J. 2004. Fractal dimension on image processing. 4th KEPAF Conference on Image Analysis and Pattern Recognition. Vol.4, pp.20.

Berke, J. 2006. Measuring of Spectral Fractal Dimension, Advances in Systems. Computing Sciences and Software Engineering. Springer pp. 397-402., ISBN 10 1-4020-5262-6.

Berke, J. 2007. Measuring of Spectral Fractal Dimension. *Journal of New Mathematics and Natural Computation*. ISSN 1793-0057, 3/3: 409-418.

Berke, J. 2008. A Spektrális fraktálszerkezet vizsgálatának elméleti és gyakorlati lehetőségei. Informatika a Felsőoktatásban 2008 Konferencia. Debrecen. ISBN 978-963-473-129-0.

Berke, J. und Kozma-Bognár, V. 2008. Fernerkundung und Feldmessungen im Gebiet des Kis-Balaton I.. Moorschutz im Wald / Renaturierung von Braunmoosmooren. Lübben.

Berke, J., Hegedűs, Gy. Cs., Kelemen, D. and Szabó, J. 2004. Digital image processing and applications. 128-142 pp. ISBN 963 00 5744 1.

Broge, N. H. and Mortensen, J. V. 2002. Deriving green crop area index and canopy chlorophyll density of winter wheat from spectral reflectance data. *Remote Sensing of Environment.* 80. 45–57.

Burai, P. 2006. Első magyarországi légi hiperspektrális képalkotó rendszer AISA DUAL, 4. Fény-Tér-Kép Konferencia, Dobogókő.

Burai, P. 2007. Távérzékelési módszerek összehasonlító elemzése mezőgazdasági mintaterületeken. Debreceni Egyetem, Agrártudományi Centrum, Mezőgazdaságtudományi Kar, Víz- és Környezetgazdálkodási Tanszék. PhD dolgozat.

Busznyák, J., Nagy, G. és Berke, J. 2008. Georgikon GNSS bázisállomás üzembehelyezésének tapasztalatai. Informatika a Felsőoktatásban 2008 Konferencia, Debrecen. ISBN 978-963-473-129-0.

Clevers, J.G.P.W., De Jong, S.M., Epema, G.F., Van Der Meer, F.D., Bakker, W.H., Skidmore, A.K. and Scholte, K.H. 2002. Derivation of the red edge index using the MERIS standard band setting. *International Journal of Remote Sensing.* 23 (16), 3169–3184.

Hargitai, H. 2006. A hiperspektrális képfeldolgozás módszerei és az első magyarországi képalkotó spektrométeres repülés adatainak elemzése. ELTE TTK FDI. PhD dolgozat.

Hexium Műszaki Fejlesztő Kft. Hexium hordozható hőkamera: HX-IDS-M 110. www.hexium.hu .

Jung, A. 2005. Spektrális információk alkalmazása a városklíma-kutatásban. Budapesti Corvinus Egyetem Kertészettudományi Kar, Kertészettudományi Doktori Iskola. PhD. Dolgozat.

EU Council, 149/2003/EK belső rendelet.

Kozma-Bognár, V., Hegedűs, G. and Berke, J. 2007. Fractal texture based image classification on hyperspectral data. AVA 3 International Conference on Agricultural Economics, Rural Development and Informatics. Debrecen. ISBN 978-963-87118-7-8.

Kozma-Bognár, V. 2008. Hiperspektrális felvételek mezőgazdasági és környezetvédelmi célú felhasználásának lehetőségei a Keszthelyi térségben. Informatika a felsőoktatásban 2008 Konferencia. Debrecen. ISBN 978-963-473-129-0.

Kozma-Bognár, V., Hermann, P., Bencze, K., Berke, J. and Busznyák, J. 2008. Possibilities of an Interactive Report on Terrain Measurement. *Journal of Applied Multimedia*. No. 2/III./2008. pp. 33-43., ISSN 1789-6967.

http://www.jampaper.eu/Jampaper_ENG/Issue_files/JAM080202e.pdf.

Kozma-Bognár, V., Kovács, ZS., Berke, J. 2008. 8 bit or 16 bit, 6th Fény-Tér-Kép Conference, Dobogókő.

Mandelbrot, B. B. 1983. The fractal geometry of nature. W.H. Freeman and Company. New York.

Mutanga, O. and Skidmore, A. K. 2004. Integrating imaging spectroscopy and neural networks to map grass quality in the Kruger National Park, South Africa. *Remote Sensing of Environment.* 90 (2004) 104– 115.

Nagy, A., Tamás, J., Burai, P. és Lénárt, CS. 2008. Hiperspektrális távérzékelés szerepe. Informatika a felsőoktatásban 2008 Konferencia. Debrecen. ISBN 978-963-473-129-0.

Peitgen, H-O. and Saupe, D. 1988. The Science of fractal images. Springer-Verlag. New York.

Sabins, F. F. 1987. Remote Sensing. Principles and Interpretation. W. H. Freeman and Co. Los Angeles. ISBN 0-7167-1793-X.

Schowengerdt, R. A. 2007. Remote Sensing Models and Methods for Image Processing. Elsevier. ISBN 13: 978-0-12-369407-2.

SFD official website: www.digkep.hu\sfd\index.htm

Specim Spectral Imaging LTD. CaliGeo software. http://www.specim.fi/media/pdf/aisa-datasheets/caligeo-ver1-07.pdf

Tamás, J. és Róth, L. 2008. Hiperspektrális adatfeldolgozási és megjelenítési lehetőségek. Fény-Tér-Kép 2008 konferencia. Dobogókő.

USGS Digital Spectral Library. http://speclab.cr.usgs.gov/spectral-lib.html.

Varshney, P. K. and Arora, M. K. 2004. Advanced Image Processing Techniques for Remotely Sensed Hyperspectral Data. Springer-Verlag. New York.

LOCAL POWER SUPPLY BY USING WOOD CHIPS - EXPERIENCES IN CONSTRUCTING AND OPERATING A BIOMASS FURNACE

Kornél Németh

Pannon University, Georgikon Faculty of Agriculture,

Department of Agricultural Engineering and Farm Mechanisation,

Keszthely

E-mail: nemethkornel@freemail.hu

Abstract

The utilization of renewable energy sources considerably contributes to the development of power supply in Hungary, which is caused by the growing energy prices, certain issues on environmental protection, and the efforts to reduce energy dependency.

In the future traditional fuels can be replaced by biomass mainly - such as main and secondary products of animal breeding or forestry -, due to its comprehensive utilization possibilities and the ability of continuous reproduction. Finally, we have the proper technologies to exploit them. In order to apply them in the most profitable way, we have to use them in the place of production or in its close area.

This study examines decentralized power generation, especially the utilization of wood chips. The research focuses on match wood burning as a possibility of local power supply and reveals its effects on the economy, society, and environment. Practical application of the data collected during the survey can reduce the energy dependency of a given area, moreover, the whole country, thus create an environmental friendly and sustainable energy management.

Keywords: renewable energy sources, biomass utilization, burning wood chips

Összefoglalás

A magyarországi energiaellátás fejlesztési feladatai között fontos szerepet kap a megújuló energiaforrások minél szélesebb körben való alkalmazása. Ezt elsősorban az energiaimport függőség csökkentése, a környezetvédelmi szempontok érvényesítése és a növekvő energiaárak indokolják.

A jövőben a hagyományos energiahordozók kiváltásának legígéretesebb megoldását hazánkban a mezőgazdaság által nagy tömegben újratermelhető növényi eredetű biomassza-féleségek, a mezőgazdasági és erdőgazdasági melléktermékek kínálják. Hasznosításukhoz ma már megfelelő technológiák állnak rendelkezésre. Gazdaságos alkalmazásuk leginkább az előállítás helyén, illetve ahhoz közeli vidéki térségekben valósulhat meg.

A vizsgálat a decentralizált energiatermelés kérdéskörét tekinti át, melyben a különböző biomassza féleségek közül fontos szerephez juthat a jövőben a faapríték hasznosítás. A vizsgálat során a faapríték hasznosítással megvalósuló települési szintű energiatermelés gazdaságra, társadalomra és környezetre gyakorolt hatásaira keressük a választ. A kutatás során felhalmozódó gyakorlati tapasztalatok elősegíthetik egy-egy térség, régió, és ebből adódóan az ország energiafüggőségének csökkentését és egy környezetbarát és fenntartható energiagazdaság megteremtését.

Kulcsszavak: megújuló energiaforrások, biomassza hasznosítás, faapríték tüzelés

1. Introduction

In March 2007 the Council of the European Union sanctioned an objective to increase the quantity of renewable energy sources up to 20 per cent by 2020 in proportion to 1990, while the emission of greenhouse gases should be reduced by 20 per cent.

In present-day Hungary the ratio of renewable energy sources to total energy consumption is about 3,8-4 per cent (Tóvári and Körmendi, 2007). Both Hungarian energy policy and issues in the topic urge to extend the use of biomass as a renewable energy source. Raising the percentage is important in fulfilling the objectives set up by EU; furthermore there is a chance to exploit farm lands in order to decrease energy import. (Bohoczky, 2007).

Energy from biomass can be employed in rural areas mainly. Local power supply based on biomass energy pares down shipping, storage, and distributional charges, while it remains competitive with fossil resources (Bai, 2007).

Wood chips burning is to become the most vital way of providing energy for minor settlements and bureaux. Many are the examples from Germany, Austria, or Denmark, where hundreds of wood chipping furnaces were built in the last 15 years. These heating plants utilize fuels that are developed locally, so the money assigned to power generation falls to the district's share. According to rough estimates, in Burgenland (province in Austria) the finances gained by applying ca. fifty local stokers using biomass energy are equal to the total value of capital investment (Garai and Riebenbaurer, 2007). Hopefully, in the near future Hungary will set up this new and efficient procedure in rural development, too.

For the moment, in our country chips burning is limited to the areas where there is none, or insufficient gas network. However, it can be successful in districts with gas network as well: prices are increasing while the assistance system is changing, therefore people will soon realize the advantages of this fresh method (Kovács, 1995).

2. Material and Methods

The present study analyzes the technical and service data of a heating plant set up in Pornóapáti in 2005. The stoker employs wood chips. The energy for heating and domestic hot water preparation in the

village is provided by the plant. The purpose of this process is to supply energy for family houses, industrial units and institutions in an environmental friendly way.

Energy resources of biomass origin meet the following requirements in order to apply them properly in energy systems: base material with appropriate quality and suitable application engineering. In Hungary woods chips for burning are not standardized yet, so one has to examine trade sources carefully before they choose the matching combustion equipment and technology.

Experts improve efficiency and measurement methods by continuously analyzing and normalizing the technology. When summarizing the advantages of utilizing biomass in energetics we have to consider certain environmental, economic, and social points of view; the issue of renewable energy sources and these three factors have to be treated and solved together.

3. Results

3.1 Application engineering and base material supply

Pornóapáti set the objective to supply power for the community by establishing a service that is environmental friendly, profitable and improves the quality of life. The local authorities and the inhabitants agreed to construct a heating plant burning wood chips. In the villages of Austria such methods function properly, and the people living in the border region see, know, and accept these technologies.

The heating plant's success consists of many elements: no gas network was created in the vicinity, but there was large quantity of biomass (wood chips), what is more the village won financial assistance in 2005. The project contains three essential parts: the heating plant, the thermal transmission line network, and the heat centres.

The heat energy is provided by two 600 kW combustion equipments using up wood chips and industrial waste-chip. The insulated, buried thermal transmission lines are 3900 metres long altogether. The consumers are equipped with the so-called heat centres that convey the energy to the heating and domestic hot water circuits.

The settlement has 136 family houses; during the construction stage 104 proprietors indicated their intention to join the network. The expected energy demand was calculated respecting the fact that nine public institutions and some local industrial units was to connect as well.

In order to determine the proper dimension of a central heating apparatus experts have to be aware of the heat demand. Since no data existed about the heat energy consumption of the houses, it was calculated by applying a variety of figures e.g. thermal insulation, structural features, or how old the building is. Table 1 summarizes the facts about the potential consumers.

Table 1: Output and heat demand as estimated in the construction period.

	Output demand (kW)	Heat demand / year (GJ)	Domestic hot water demand / year (GJ)
Institutions	135	729	88
Inhabitants	1120	6402	894
Industrial units	121	760	20
Total	**1376**	**8378**	**1002**

Energy demands are significantly influenced by thermal factors in the heating season. Under typical conditions the estimated value of heat demand is 9380 GJ in a year; this is the total amount of demand for heating and domestic hot water preparation. In order to transmit the proper quantity of heat to the consumers, more energy has to be applied in the system than the estimated amount, because energy is lost e.g. in the heating plant itself (15%), in the thermal transmission lines (4%), and in the heat centres (4%). Considering these figures it turned out that the heat demand is 12096 GJ in a year, so the output of the combustion equipment has to be 1200 kW.

Fuel demand is described as a ratio of the heat demand in a year (12096 GJ) and the heating value of a combustible. The heating value of wood chips varies by moisture, but we can calculate the actual value by using the following formula (Kacz and Neményi, 1998):

$$H_w = \frac{H_{w=0}(100\text{-}w) - 2.44 \cdot w}{100} \qquad [MJ/kg]$$

where H_w - *w* indicates the heating value of moist wood (MJ/kg)

$H_{w=0}$ - heating value of dry wood (*w* = 0) (MJ/kg)

w - moisture (%)

2.44 - enthalpy of vaporization of water at 25°C (MJ/kg)

Moisture content of stored chip is about 25-35%. Taking its average (30%) into consideration we can express the heating value this way:

$$H_{30\%} = \frac{19 \cdot (100\text{-}30) - 2.44 \cdot 30}{100} = 12.5 \text{ MJ/kg}$$

It be as much as saying that the heating value of wood chips with 30% moisture content is 12.5 MJ/kg; therefore the fuel demand is (12096/12.5) 968 tons/year. This quantity is provided by industrial units, the forest (111 acres) near the village, or any other external source of supply.

3.2 Effects on the environment and the society

When producing, processing and using solid biomass we have to be sure that we bring about the least environmental pollution. To do so, we have to minimize the emission of greenhouse gases and other harmful pollutants during the production, transportation and utilization.

The most notable effects of heating centres utilizing renewable energy sources on the environment means that no emission is produced by fossil fuels any more, because they are replaced with a well-regulated central system. Table 2 summarizes the projected

replacements in Pornóapáti considering the amount of traditional energy sources.

Table 2: Quantity of fossil fuels replaced by renewable energies

Energy resources	Projected replacement
Coal	347 t/year
Fuel wood	260 t/year
PB-gas	4.9 t/year
Electric energy	370 MWh/year

Emission is reduced mainly by substituting coal and fuel wood burning with the new technology. Electric energy is saved as well, since domestic hot water is prepared in the heating plant.

The rate of emission is much lower when burning matchwood than using the so-called traditional heating systems. It is mainly because of the chemical components of the raw material and the specific formation of the stokehold. At the same time we have to be aware of an additional emission concerning pollutants like NOx or dust.

The emission of stokers with output 140 kW – 50 MW is restricted by law [23/2001 (13.11.) Instruction of KÖM]. The statute declares that the extent of emission has to be monitored by the service provider once in a year; at his own expense he is bound to entrust an organisation determined by law with doing the measuring. Table 3 compares the predetermined threshold limits and the actual values computed by the Hungarian Institute of Agricultural Engineering in Pornóapáti in December 2006.

Table 3: Limits of emission and actual values measured in Pornóapáti

Air pollutants	**Threshold limits [mg/m^3]**	**Actual values Furnace 1. [mg/m^3]**		**Actual values Furnace 2. [mg/m^3]**	
		50% rate of charging	100% rate of charging	50% rate of charging	100% rate of charging
Solid material	150	128.9	131.6	145.0	140.2
Carbon monoxide (CO)	250	23.1	119.4	64.4	116.9
Nitrogen oxides (in terms of NO_2)	650	142.3	125.2	158.9	100.8
Sulphur dioxide and sulphur trioxide (in terms of SO_2)	1000	114.1	90.3	135.0	76.3
Unburnt organic carbon compounds in terms of coal	50	2.6	31.9	19.5	26.2

Source: My own table based on the data provided by 23/2001 (XI.13.) KöM rendelet and the report of Hungarian Institute of Agricultural Engineering, 2006

The concentrations above (unit: mg/m^3) mean flue gases with 11 per cent oxygen content. Built-in elements (dust and waste gas filter) and the use of chemical-free base material assure that the regulations will not be violated.

Projects like this contribute to rural development. They bring about progress in infrastructure and employment, increase capital investments, while people living in a clean, ordered environment will form a rounded whole. The time one spends to supply power for the household will decrease, thus individuals will have more and more

spare time, which plays an important role in bettering the quality of life.

Promoting environmental protection and environmentally conscious attitude involves providing large-scale information about the utilization of renewable energy sources in an efficient way. The most notable effect of the project lies in its capability to form people's attitude and make them change their minds, though this outcome can hardly be illustrated with numbers. The experiences gained during the construction and operation processes can break new grounds and help evolve a specific branch of rural development in Hungary.

Someday there will be demand for energy plants which gives rise to a more reasonable utilization of soil and the production of marketable commodities. The establishment of energy crops would also be a possible solution for the problems of over-production and marketing.

Activities associated with the exploitation of renewable energy sources (e.g. agriculture, transportation, trade, industrial processing) may create new work opportunities in a given region, contribute to expand the income-earning facilities in rural areas and increase the population-retaining capacity of settlements.

4. Discussion

The exploitation of biomass may provide safe power supply, reduce energy dependency and help establish sustainable development and sustainable energy management in Hungary.

Wood chips burning is the only one of the possible methods for local power supply. In the surrounding countries we can see many examples for this modern, environmental friendly and efficient way of biomass utilization. In Hungary we have to choose carefully the place for these new models and technologies, because a wrong decision may hinder the success of other projects for years.

We can tell that in Pornóapáti the heating plant functions properly and this long-term investment can be maintained, since biomass energy is competitive with the actual costs of fossil resources.

Base material supply is uninterrupted in the heating plant, because the required quantity of wood chips (1000 tons/year) is available at a fair price. The fully automatic application technology meets the environmental regulations and points of view.

Unfortunately, in our country efforts to utilize biomass or other renewable energy source are suppressed by the existing infrastructures (e.g. gas network). Licensing procedures are usually long and complicated. In spite of all these facts, the ratio of renewable energy exploitation will increase in the near future, since fossil fuels are more expensive but less available.

References

Bai A., 2007. A biogáz (Biogas). Száz magyar falu könyvesháza Kht, Budapest, 201-202.

Bohoczky F., 2007. Az agrárium helye az energiafejlesztésben (The role of agriculture in energy development). *Agrárium, agrár- és piacgazdaság.* **10.** 24.

Garai Zs., Riebenbaurer L., 2007. Falufűtőművek története Ausztriában (History of heating plants in Austria). Bioenergia-Energetikai szaklap. **5.** 30.

Kacz K., Neményi M., 1998. Megújuló energiaforrások (Renewable energy sources). Mezőgazdasági Szaktudás Kiadó, Budapest. 103.

Kovács A., 1995. Faapríték tüzelés (Wood chip burning). Phare kiadvány. Energia Központ Kht. *Csináljuk jól*. **7.** 17.

Németh G., 2007. Faapríték tüzelés a szombathelyi távfűtésben (District heating in Szombathely using wood chips). *Magyar Energetika.* **6.** 26.

Tóvári P., Körmendi P., 2007. Szilárd biomassza tüzeléstechnikai alkalmazásának lehetőségei Magyarországon (Chances for using solid biomass in combustion engineering in Hungary). *Agrárágazat.* **7.** 67.

EXAMINATION OF EYE IRRITANCY BY USING THE CHORIOALLANTOIS MEMBRANE OF THE HEN'S EGG

Judit Tavaszi and Péter Budai

University of Pannonia, Georgikon Faculty

Institute of Plant Protection Department of Hygiene

Keszthely, 16 Deák F. Str.

tavaszi.judit@2000.georgikon.hu

Summary

Agrochemicals must undergo numerous toxicological tests before registration. One of these experiments is the examination of eye irritation potential. To get knowledge about eye irritation, nowadays only the *in vivo* Draize-test is accepted, which is one of the most criticized methods because of the injuries inflicted on the test animals. Because of this fact, several various in vitro tests have been developed to replace the rabbits in detecting the irritation potential of chemicals. One of these alternative methods is the HET-CAM test, which uses the chorioallantoic membrane (CAM) of the embrionated chicken egg.

In our studies comparative screening was performed with a set of agrochemicals to establish paralell data on in vitro (HET-CAM) and in vivo (Draize) results in the case of 12 liquid agrochemicals. The solutions to be tested are added to the membrane and left in contact for 5 minutes and the membrane is examined for vascular damage at set

time periods. Irritancy is scored according to the severity and speed at which damage occurs providing an indication of the likely irritant effect of the compound.
Our study showed good correlation between results obtained by the HET-CAM test and those of the Draize rabbit eye test in most cases. The present form of the HET-CAM test can be proposed as a pre-screen method of eye irritation tests.

Keywords: in vitro, HET-CAM, eye irritation

Összefoglalás

A mezőgazdasági vegyi anyagok forgalomba hozatalát napjainkban számos toxikológiai vizsgálat előzi meg. Ezek a vegyszerek olyan tulajdonságait tárják fel, amelyek a humán egészségkockázat jellemzéséhez szükségesek. A szemirritáció mértékének meghatározására jelenleg a Draize-féle nyúlon elvégzett tesztből származó eredményeket fogadják el, de az erősödő állatvédő mozgalmak hatására több olyan in vitro módszer is kidolgozás alatt áll, amely nem csak csökkentheti az emlős kísérleti állatok számát, hanem esetleg teljes mértékben ki is válthatja ezek felhasználását. A persektivikus alternatív módszerek közé tartozik a jelen vizsgálatban alkalmazott, a tyúktojás chorioallantois membránját (CAM) használó

HET-CAM teszt. Az in vitro módszerrel kapott eredményeket a Draize-féle vizsgálatból származó in vivo adatokkal vetettük össze.
A kísérletekben 11 folyékony növényvédő szert és 1 növény-tápoldatot használtunk fel.

A HET-CAM teszt elvégzésekor mindegyik vizsgálati anyagot 100%-os koncentrációban alkalmaztuk. A tojásokat 70 %-os páratartalom mellett 37 ^{o}C-on keltettük, 9 napon át napi gyakorisággal forgattuk, hogy elkerüljük az embrió letapadását. A 10. napon, lámpázás után a hibás tojásokat eltávolítottuk, majd előkészítés után a chorioallantois membránra cseppentettük a vizsgálati anyagokat. A kezelést minden esetben 4 alkalommal, 6 ismétlésben végeztük el. A CAM-on jelentkező elváltozásokat és a változások megjelenési időpontjait másodpercekben rögzítettük, majd ezekből irritációs indexeket számoltunk. A klasszikus Draize-féle szemirritációs vizsgálatot 405-ös számú OECD Guideline alapján végeztük el.

A vizsgálataink során felhasznált kísérleti anyagok in vitro irritációs indexei jó korrelációt mutattak az in vivo adatokkal. Az in vitro HET-CAM teszt számos előnnyel rendelkezik az in vivo módszerekkel szemben. Olcsóbb és gyorsabb, mint a Draize-féle vizsgálat, ugyanakkor eredményei jól közelítik az in vivo adatokat. Hátránya a szubjektivitás, ami miatt leginkább más in vitro tesztekkel kombinálva lehet alkalmas az in vivo vizsgálatok kiváltására. Nagy érzékenysége miatt, mint elővizsgálat javasolható.

Introduction

Nowadays, all chemicals have to be tested before putting into circulation. In this process toxicological examinations play an important role, because they can show several features of the ingredients, which preclude the possibility of manufacturing. To determine the ocular irritation, only the Draize rabbit eye test is accepted now. Because of the pain caused on the test animals, many alternative methods have been developed to replace rabbits in the future. most of these methods are in process of validation now.

The HET-CAM test, using the chorioallantoic membrane (CAM) of the chicken egg, is one of the possible suggested alternatives (Walum et al., 1992). The chorioallantoic membrane has been used extensively for many years in various fields of biological research. With arteries, capillaries and veins, the CAM can be regarded as a complete tissue. It is technically easy to study and responds to injury with inflammatory reaction, similar to the rabbit's eye (Leighton et al., 1985). The potential irritancy of compounds may be detected by observing adverse changes, which occur in the chorioallantoic membrane (CAM) of the egg after to test chemicals. During the test the chemicals are placed directly onto the chorioallantoic membrane. The changes of the vascular injury (haemorrhage, lysis) or coagulation in response to a compound is an indication of the potential of the chemical to damage mucous membranes. In our experiment 12 fluid agrochemicals were evaluated by the HET-CAM test. The results were compared with *in vivo* data from Draize eye irritation test.

Materials and methods

Test materials

The test preparations included Previcur 607 SL (Propamocarb-hydrochlorid), Charisma 207 EC (Famoxadone), Substral, Unifosz 50 EC (Dichlorfos), Confidor SL 200 (Imidachloprid), Fozát 480 (Glifozat izopropilamin), Systhane 12 E (Myclobutanil, cyclohexanone), Sumi-Alpha 5 EC (Esfenvalrate), Agrol, Topas (Penkonazol), Omite 57 E (Propargite), and Chinmetrin (beta-cypermethrin).

Agrochemicals were tested in all cases at 100% concentrations.

HET-CAM test

The CAM is a complete tissue including arteries, capillaries and veins, and is technically easy to study. It responds to injury with a complete inflammatory reaction, similar to the tissue of the rabbit eye.

The potential irritancy of compounds may be detected by observing adverse changes, which occur in the chorioallantoic membrane (CAM) of the egg after testing chemicals. During the test the chemicals are placed directly onto the chorioallantoic membrane. The occurrence of vascular injury or coagulation in response to a compound is the basis for employing this technique as an indication of the likelihood that a chemical would damage mucous membranes (especially the eye) *in vivo*.

Shaver rusticbrow chicken eggs were used. Before testing eggs were candled and any defective were discarded. The eggs were incubated in a Ragus incubator. The temperature was 37 ^{o}C and relative humidity was 70%. Eggs were rotated for 8 days to prevent the attachment of the embryo to one side of the egg. They were candled on the 9th day and any non-viable were discarded. The eggs were replaced into the incubator with the large end upwards but were not rotated, accessibility to the chorioallantoic membrane was ensured in this way. On the 10th day they were prepared for assaying. The air cells were marked and the section of shell was removed with scissors. The membrane was moistened carefully with 0.9 % NaCl solution and eggs were replaced in the incubator until ready for assaying.
Standards were prepared directly before each assay.

Standards: 2 eggs with 1 % Sodium dodecil sulphate and 0.1 M NaOH.

Controls: 2 eggs with 0.9 % NaCl.

Test: 6 eggs treated with pesticide

All test solutions were run on 4 separated replicates.
The membrane was removed carefully with tapered forceps. 0.3 ml of test fluid was added to the chorioallantoic membrane and the effect was observed over a period of 5 minutes. On the chorioallantoic membrane hemorrhage, vascular lysis or coagulation can be seen. The times of

changes were recorded in seconds. A computer software was used to evaluate data (Invittox Protocol no. 47).

The computer software uses the following algorithm:

$$RI = \frac{301\text{-}secH}{300} \times 5 + \frac{301\text{-}secL}{300} \times 7 + \frac{301\text{-}secC}{300} \times 9$$

Where H = haemorrhage, L = vascular lysis, C = coagulation, RI = irritation index, and sec = start second.

Draize Rabbit Eye Test

In our experiment 3 New-Zealand albino rabbits were used in each assay. The use of separated control group is not necessary, the untreated eye serves as control. Rabbits were kept in the separate cages of a climatic animal room. The temperature was 22-25 ^{o}C and relative humidity was 50-70 %. Laboratory rabbit food was given for food, and tap water was served to drink ad libitum.

A volume of 0.1 ml agrochemical was instilled into the conjunctival sac of each rabbit. Ocular irritation was evaluated at 1 hour, 1, 2, 3, 4 and 7 days post installation (Draize et al., 1944). Individual scores were recorded for each animal. The time interval with the highest mean score (Maximum Mean Total Score – MMTS) for all rabbits was used to classify the test substance by the system of Kay and Calandra, (1962). The results can be seen in Table 4.

Results

Results from the HET-CAM test

The numerical data are summarised in Table 1. During the 5 min period of observation after treatment with the test pesticides the following changes were seen.

Table 1 Irritation indices from HET-CAM test

Test materials	Irritation index
Previcur 607 SL	4.70
Charisma 207 EC	4.02
Substral	4.80
Unifosz 50 EC	4.96
Confidor 200 SL	4.92
Fozát 480	4.94
Systhane 12 E	11.50
Sumi-Alpha 5 EC	10.80
Agrol	4.80
Topas	11.55
Omite 57 E	10.21
Chinmetrin	11.70
SDS 1 % + NaOH 0.1 M	11.53

Using the Previcur 607 SL, slight haemorrhage occured between 13 and 25 sec after treatment. The irritation index showed Previcur 607 SL to be a weak irritant.

After treatment with Charisma 207 EC, slight haemorrhage started in 9th sec after treatment. On the basis of the irritation index calculated from the observed changes with the help of a computer software, Charisma was a weak irritant at a concentration of 100%.

When Substral was used, slight haemorrhage started in 10 to 16 sec after treatment. The irritation index showed Substral to be a weak irritant in this concentration.

The Unifosz 50 EC caused slight haemorrhage that occured in 8 sec after treatment. On the basis of the irritation indices, this pesticide is a weak irritant.

When Confidor SL 200 was used, slight haemorrhage started in 8 to12 sec after treatment. The irritation index showed Confidor SL 200 to be a weak irritant in this concentration.

The treatment of eggs with Fozát 480 induced slight haemorrhage that started in 10th sec. On the basis of the irritation indices, the pesticide is a weak irritant.

After the treatment with Systhane 12 E lysis was observed between 5 and 12 sec, and haemorrhage between 14 and 28 sec. By these results this pesticide is severely irritative.

The Sumi-Alpha 5 EC resulted mild haemorrhage after 2 to 7 sec. The irritation index showed Sumi-Alpha 5 EC to be a moderate irritant.

Using Agrol, slight haemorrhage occured between 9 and 17 sec after treatment. On the basis of the irritation indices, the pesticide is a weak irritant.

Topas caused lysis started 5 to 10 sec and followed by haemorrhage between 14 and 21 sec after treatment. On the basis of the irritation indices, this pesticide is severely irritative.

The treatment of eggs with Omite 57 E induced lysis between 20 and 43 sec, and haemorrhage that started 45 to 77 sec after

treatment. The irritation index showed Omite 57 E to be a severe irritant.

Chinmetrin resulted lysis between 3 and 7 sec after treatment, and mild haemorrhage after 9 to 16 sec. The irritation index showed Chinmetrin to be a severe irritant.

The obtained irritation indices can be evaluated by using the classification categories of Table 2.

Table 2 Classification categories of HET-CAM test

Irritation index	Irritation category
0-0.9	no irritation
1-4.9	weak irritation
5-8.9	moderate irritation
9-21	severe irritation

Results from Draize-test

The obtained numerical data are summarised in Table 3.

Table 3. Irritation indices from Draize-test

Test material	Irritation index	Category
Previcur 607 SL	14	Minimally
Charisma 207 EC	10	Mildly
Substral	3.3	Minimally
Unifosz 50 EC	19	Moderately
Confidor 200 SL	12.67	Mildly
Fozát 480	13	Mildly
Systhane 12 E	81	Maximally
Sumi-Alpha 5 EC	74	Extremely
Agrol	15.3	Mildly
Topas	75	Extremely
Omite 57 E	85	Maximally
Chinmetrin	85	Extremely

Slight redness for 1 hour, slight chemosis for 1 day and moderate discharge for 1 day were noted post instillation of Previcur 607 SL. Iritis did not change. On the cornea no opacity was noted during the observation period. On the base of irritation index Previcur 607 SL was minimally irritative to the rabbit eye.

Moderate redness, slight chemosis and moderate discharge were noted in the first 2 days post instillation of Charisma 207 EC. Iritis did not change. On the cornea no opacity was noted during the observation period. On the base of irritation index Charisma 207 EC was minimally irritative to the rabbit eye, but as the eyes did not return to normal in 48 hours, this chemical is mildly irritant.

Moderate redness and slight chemosis were noted in the first hour post instillation of Substral. After 24 hours the treated eyes returned to normal. Iritis did not change. On the cornea no opacity was noted during the observation period. On the base of these results, Substral was minimally irritative to the rabbit eye.

Slight redness, moderate discharge and severe chemosis were observed after treatment with Unifosz 50 EC. Iritis changed in the first hour, but in 2 days it returned to normal. There was no opacity on the cornea. As the eyes do not returned to normal until the end of the observation period, this chemical is moderately irritative.

Slight redness for 4 days, slight chemosis for 3 days and moderate discharge for 2 days were noted post instillation of Confidor 200 SL. Iritis did not change. On the cornea no opacity was noted during the observation period. On the base of irritation index Confidor

200 SL was minimally irritative, but as the symptoms were observed until the 4th day, the agrochemical is mildly irritative to the rabbit eye.

Slight redness, slight chemosis and moderate discharge were noted in the first 3 days post instillation of Fozát 480, after 3 days the treated eyes returned to normal. Iritis did not change. On the cornea no opacity was noted during the observation period. On the base of the observations Fozát 480 was mildly irritative to the rabbit eye.

After instillation of Systhane 12 E, positive conjunctival responses with severe redness, severe chemosis and strong discharge were noted until the end of the observation period.. Iritis changed in 1 hour. On the cornea moderate opacity was noted from the first day, which was observed for 7 days. On the base of irritation index Systhane 12 E was maximally irritative to the rabbit eye.

Positive conjunctival responses with moderate redness, strong chemosis and strong discharge were noted post instillation of Sumi-Alpha 5 EC. Iritis changed in 1 day. On the cornea moderate opacity was noted from the first day until the end of the observation period. On the base of irritation index Sumi-Alpha 5 EC was extremely irritative to the rabbit eye.

Severe redness, moderate discharge and strong chemosis were noted after treatment with Agrol. The iritis and the cornea did not change. The eyes returned to normal in 72 hours. With the irritation index of 15.3, Agrol is mildly irritative.

Severe redness, chemosis and strong discharge were noted during the observation post instillation of Topas. Iritis changed on the first day, and did not return to normal in the case of 2 rabbits. On the

cornea moderate opacity was noted from the first hour until the end of the observation period. On the base of irritation index Topas was extremely irritative to the rabbit eye.

After treatment with Omite 57 E severe redness, severe chemosis and strong discharge were noted during 7 days. Iritis changed from the first day and it was permanent during the observation period. On the cornea strong opacity was noted from 1 hour in the case of one animal and from the first day in the case of the other two animals, until the end of the observation period. On the base of irritation index Omite 57 E was maximally irritative to the rabbit eye.

Positive conjunctival responses with severe redness, chemosis and strong discharge were noted during the observation post instillation of Chinmetrin. Iritis changed after 1 day. On the cornea moderate opacity was noted from the first day, and strong opacity from the 4th day until the end of the observation period. On the base of irritation index Chinmetrin was extremely irritative to the rabbit eye (Table 4).

Table 4 Classification of eye irritation scores from Draize eye irritation test

MMTS	Irritation classification
0.0 – 0.5	non
0.6 – 2.5	practically non
2.6 – 15.0	minimally
15.1 – 25.0	mildly
25.1 – 50.0	moderately
50.1 – 80.0	severely
80.1 – 100.0	extremely
100.1 – 110	maximally

Discussion

The HET-CAM test has several advantages including its rapidity, simplicity, sensitivity, ease of performance and its relative cheapness. Disadvantages of the HET-CAM test are the subjective nature of the evaluation of the results. The evaluation cannot be done in the case of opaque chemicals, because these materials cover up the membrane. To test powder or granulate formulations the rinsed method of the HET-CAM test can be used, but this is more complicated than the simple method because of the injury caused by rinsing.
The results of *in vitro* and *in vivo* tests can be seen in Table 5.

Table 5 Irritation categories by HET-CAM test in comparison to irritation categories by Draize rabbit eye test

Pesticide	Category from HET-CAM test	Category from Draize rabbit eye test
Previcur 607 SL	Weak irritative	Minimally
Charisma 207 EC	Weak irritative	Mildly
Substral	Weak irritative	Minimally
Unifosz 50 EC	Moderate irritative	Moderately
Confidor 200 SL	Weak irritative	Mildly
Fozát 480	Weak irritative	Mildly
Systhane 12 E	Severely irritative	Maximally
Sumi-Alpha 5 EC	Severely irritative	Extremely
Agrol	Weak irritative	Mildly
Topas	Severely irritative	Extremely
Omite 57 E	Severely irritative	Maximally
Chinmetrin	Severely irritative	Extremely

In several experiments a good correlation was found between the results from *in vitro* HET-CAM test and the results from *in vivo* Draize eye irritation test (Luepke and Wallat, 1987). In 1992 the

German authorities accepted the use of HET-CAM data for the classification of R41 chemicals in the notification of new industrial chemicals (Balls et al., 1999).

In this study a good correlation was also seen between the data from *in vitro* and *in vivo* methods. The HET-CAM test could not replace the currently used Draize eye irritation toxicological test, but it could diminish investigations in mammals as well as limit or eliminate pain and damage in animal experiments. In this form HET-CAM test can be useful for a pre-screen method.

References

Balls. M., Berg, N., Bruner, L.H., Curren R., deSilva, O., Earl, L.K., Esdaile, D.J., Fentem,

J.H., Liemsch, M., Ohno, Y., Prinsen, M.K., Spielmann, H. & Worth, A.P. 1999. Eye irritation testing: the way forward. The report and recommendations of ECVAM workshop 34. *ATLA* **27**. 53-77.

Draize, J.H., Woodard, G., Calvery, H.O. 1944. Methods for the study of irritation and toxicity of substance applied to the skin and mucous membranes. *J. Pharmac., exp. Ther*. **82**. 377 p. Invittox Protocol Number **47**. HET-CAM test 1990.

Kay, J.H. and Calandra, J.C. 1962. Interpretation of eye irritation tests. *J. Soc. Cos. Chem*. 1962; **13**:281-289.

Leighton, J., Nassauer, J. and Tchao, R. 1985. The chick embryo in toxicology: an alternative to the rabbit eye. *Fd. Chem. Toxic. Vol*. **23**, No. 2, 293-298.

Luepke, N.P., Wallat, S. 1987. HET-CAM reproducibility studies. *Alternative Methods in Toxicology* Vol. **5**. 353-363.

Walum, E., Balls, M. et al. 1992. ECITTS: An integrated approach to the application of *in vitro* test systems to the hazard assessment of chemicals. *ATLA*. **20**. 416.

THE USE OF ELECTRONICS AND INFORMATICS ON PLANT PROTECTION SPRAYERS

T. Sándor, M. Lönhárd, Zs. Takács, B. Pályi

University of Pannonia, Georgikon Faculty of Agriculture, Hungary, Keszthely

Department of Agricultural Engineering and Farm Mechanisation

H-8360, 7 Festetics Street Keszthely, muszaki@georgikon.hu

Abstract

The effective plant protection constitutes a basic element of the economic plant production. Beside even the most modern chemicals new techniques and methods are necessary to ensure uniform covering of the crop surface with the chemicals and by this to decrease yield losses. For these an effective tool is the using of modern information devices. Considerable amount of chemicals can be spared and decreasing of environment pollution can be achieved by using air-assisted sprayers, controlled droplet applications and target sensing techniques and site specific methods by seriousness of the infection.

Key words: plant protection, application techniques, electronic, informatics.

Összefoglalás

A növénytermelés biztonságának alapvető feltétele a növényvédelmi műveletek hatékony elvégzése. A növényvédő szerek magas fejlettségi szintje mellett elengedhetetlen a műszaki eljárások továbbfejlesztése, új korszerű technikák bevezetése, melyek célja a veszteségek csökkentése, a védendő célfelület minél jobb és egyenletesebb fedésének biztosítása. Ennek egyik hatékony eszköze a korszerű informatikai eszközök alkalmazása. Nagymértékű vegyszer-megtakarítást és a környezet terhelésének fokozott csökkentését teszi lehetővé a szélarányos, szabályozott cseppméretű permetezés, a légzsákos permetezés, a növényérzékelő permetezők, a szabályozott és helyspecifikus, fertőzés-arányos permetezési rendszerek alkalmazása.

Kulcsszavak: növényvédelem, alkalmazástechnika, elektronika, informatika.

Introduction

Further technical development methods, introduction of new techniques and modern plant protection, based on informatics can considerably promote the safety of the treatments, of its biological effectiveness and decrease the amount of pesticides and fungicides used, as well as of environment pollution. Such new techniques are the air-assisted sprayers, the controlled droplet applications, the target-sensing techniques, and the site-specific methods directed by seriousness of the infection or weed covering. Beside the survey of these technical methods and their electronic background this article presents a computerized measuring and evaluation method developed

by the Department and used for control of technical parameters of the plant protection equipments.

Site specific sprayers

Dosage regulators

By using electronic doses regulators the overdosage and underdosage of spray solution can be avoided and achieved saving of chemical amounts as much as even 30 % (Fig.1). A special measuring apparatus has been developed at our Department to investigate the regulation characteristics of dose regulators. By this the typical functions of the regulators can be determined at a given dose and at differing speed changes, independently, whether these speed changes occur within one gear or at changing the gear.

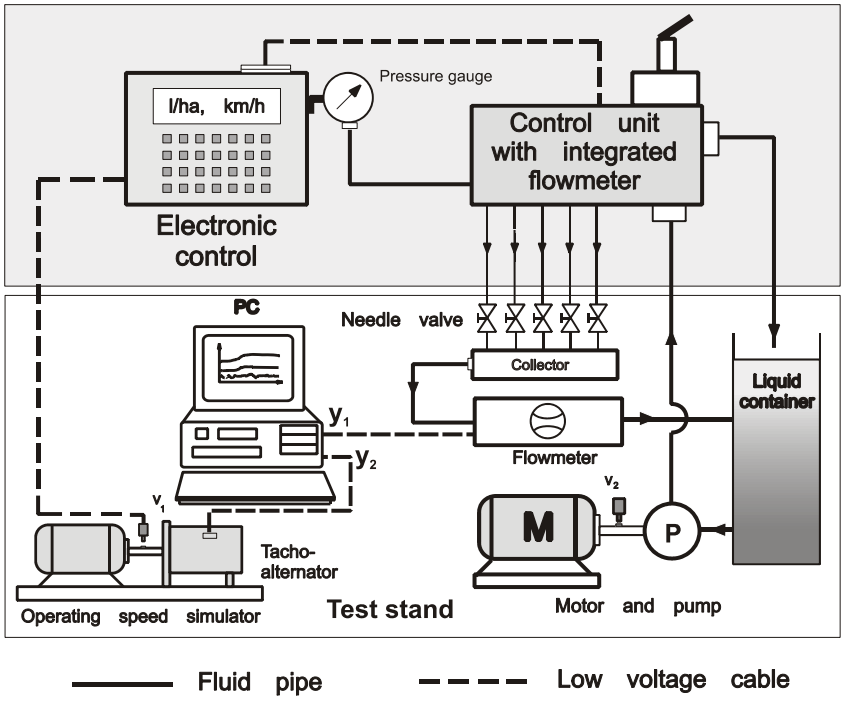

Fig. 1 The dosage regulating and measuring apparatus

Parts of the apparatus are:

- a pump mounted to an electric motor with continually-variable speed to transport fluid to the armature
- a speed simulator ,
- a collecting tube to collect spray output from parts of supposed field sprayer boom (pin valves mounted between the armature and collecting tube make possible adjusting proper cross sections ensuring desired flow speed in the supposed boom sections with given number of nozzles),
- a PC to display signals from the flow-meter speed simulator or electric motor.

To investigate dynamic characteristics of a sprayer the following changes of working situations can be simulated by changing the rotation speed of pump motor, for example at 1,5 – 2,0 – 2,5 m/s flow, or 300 l/ha amount of water:

a) start or stop of spraying,

b) speed changes within gear or at changing the gear, and

c) stop or start of different parts of the boom.

To investigate static characters using constant speed and PTO rpm the following characters can be measured:

d) repeated setting of the same volumes, and

e) accuracy of the flow meter.

From the time functions given by the PC on the display, correction time span and actual doses deviation from the nominal value can be determined.

GPS in the plant protection

The precision plant protection has three main conditions: continuous, accurate position determination, space-informatics devices, and automated work on the ground. The changing characters of the field, like weed covering or weed number has to be established or measured at different points and to find later again an accurate site-determination. This will be made nowadays by using GPS. The GPS (Global Positioning System) is now available for everybody. The system were originally planned and developed for military purposes, but soon were recognized its importance in the civil life, and as a consequence an entire industrial sector developed to produce and develop receivers, and the number of its users is continually increasing. The intention was to develop such a system, which determines different distance points on the main land or sea using the position points of the satellites. The absolute accuracy of GPS is now 15-20 m, which is good enough for navigation, but the precision plant protection needs a better accuracy, 3-5 m. The accuracy can be increased by differential measuring, by which the position of a receiver standing on an unknown point can be determined by its relation to known points. This is the differential GPS (DGPS), of which accuracy can be even a centimeter.

The parallel steering system is also a GPS-application (Fig.2). This system makes it possible moving of a machine group with its previously determined working width parallel on the field steered using given basic points.

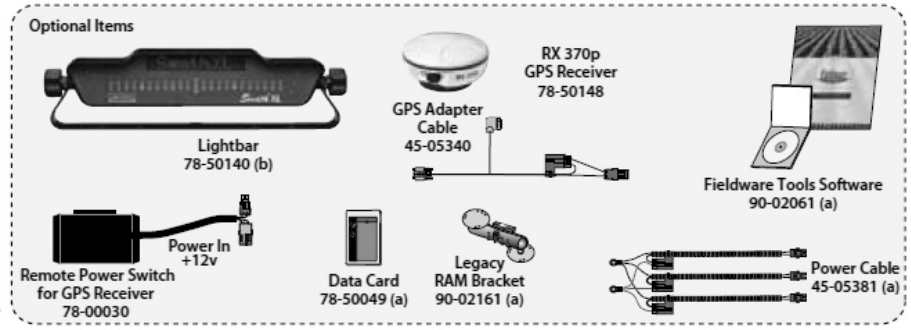

Fig. 2 Schematic overview of a parallel guidance system.

An improved version of this system is the FieldPilot (Fig.3). In this system the steering, spray regulation, and also the on/off handling of the boom is automatically running. By this the operator can pay more attention to the other critical functions, e.g. to the height of the boom, to spreading of the fluid, to the speed of the machine or to the condition of supply tank or feeder. Guidance of all functions will be made only by a single control plate and simple intuitive handling units. For full automation the steering function integrates also the steering of boom parts in order to a very accurate spraying at the end of the rows and especially at the end of point rows. When the sprayer arrives at a place sprayed before, the steering function will switch off the spraying. By avoiding the overlapping pesticide will be saved. The accuracy of the modern DGPS may be as much as even 5-25 cm.

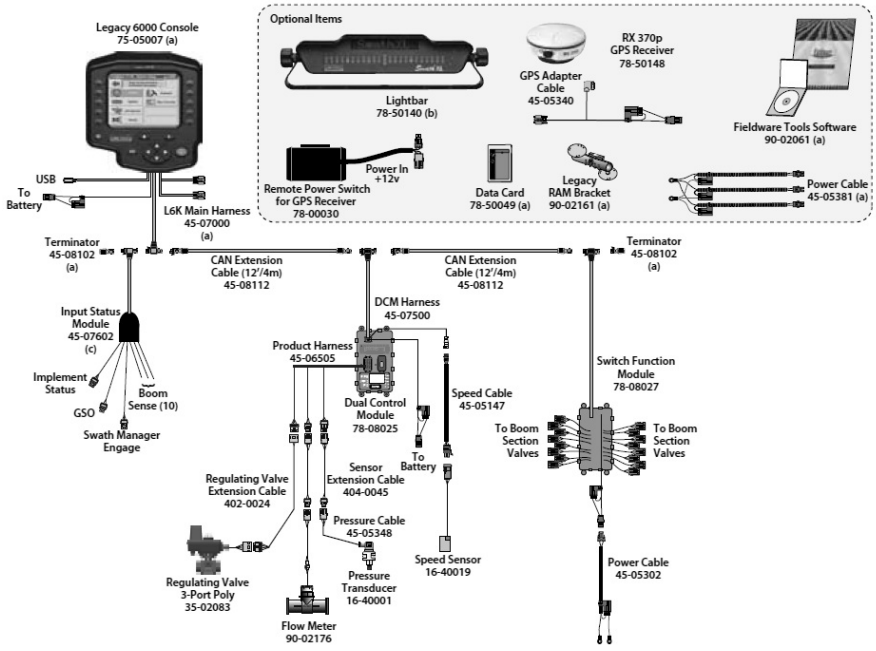

Fig. 3 Schematic overview of FieldPilot on a plant protection sprayer.

Last year (2007) a GNSS basic station (GPS, Gloness and Galileo) were established at the Georgikon Faculty of University of Pannonia. This station serves with correction data (and others) in RTK 2.1 (DGPS), RTK 2.3, and RTK 3.0 format. These corrections can be used very effectively within a distance of 50 km. Their accuracy is on geodesy level (GPS coordinates with an accuracy of a cm), its integrity amounts to 95-99 %.

GIS based pesticide application

The Geographical Information System (GIS) offers the possibility of detailed description of a field (unit of treatment) using aerial photographs and satellite receptions. By coupling these and other

information (e.g.at application of pesticides) the GIS opens new perspectives in the estimation and decrease of risks during plant protection. The GIS system and the digital image processing allow creating weed covering maps to promote site-specific plant protection. This method will be considered to be an off-line weed-sensing method. In this case first a digital aerial photograph will be produced (full area representation), which will be evaluated by an image analyzing software and then converted to a digital weed-cover map (Fig.4).

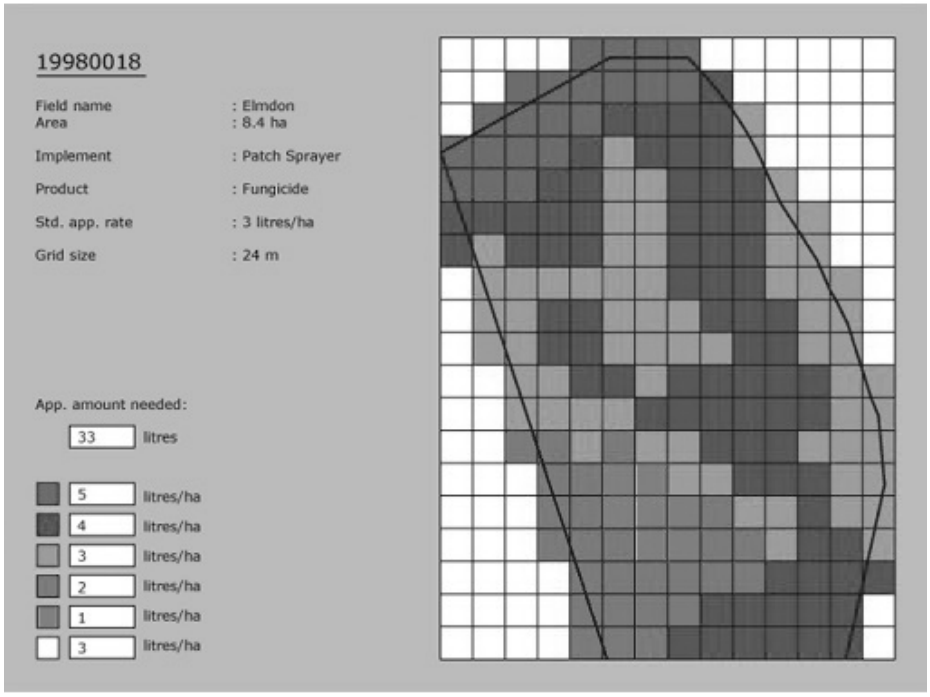

Fig. 4 Weed cover map of a field

The map can be introduced into the board of computer of the sprayer and will direct the spray only to the weed covered surfaces, to save pesticide amount.

Pesticides get their official permissions at severe conditions to minimize environment risks. This means also, that during their application certain distance to biotops (water supplies) has to be ensured to avoid environment pollution as a consequence of droplet drift. These distances are different, and depending on the chemical, it can be even 100 meters. The infringement of these rules involves penalty, and will be supervised by territorial authorities. Using GIS data the agricultural areas can be categorized with respect to applications of chemicals and of water supplies and biotops (Fig.5). Therefore 5x5 m raster cells will be created for the entire field to be sprayed, and for all cells the distances from water supplies (biotops) will be determined by the GIS functions. By this a simple GIS data collection can be served to the board computer of the sprayer machine.

Fig. 5 Digital model of a landscape unit

Using GPS first the exact location of the boom will be determined, then the distance of the biotop (water supplies) using the line code of the pesticide (automation). The nozzles can be disconnected according to this information. The possibilities of GIS usage is however wider: When the distance of cells and of water supply are considered as basic information, using data given for the chemical also a correction can be made automatically to eliminate the drift effect.

On-line pesticide feeding

The modern informatics system makes possible the site-specific treatment by direct pesticide feeding into the transport liquid. The PC-assisted automatic system considers both the moving speed of the sprayer and the weed infestation (Fig. 6). The central unit feeds the chemical according to the speed of the sprayer.

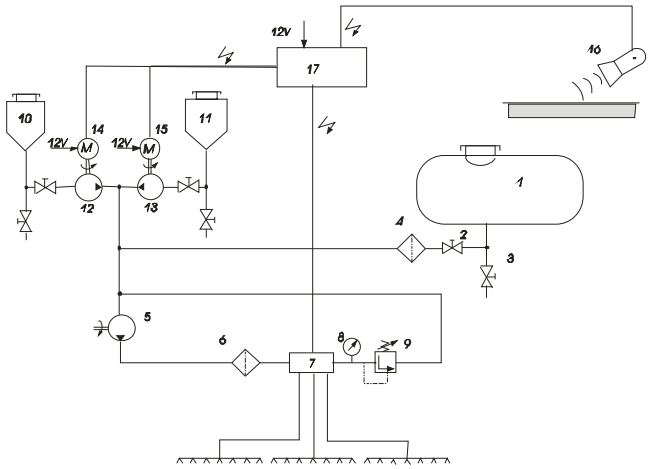

Fig. 6 On-line pesticide feeding

(1) Water tank, (2) Cut-off valve, (3) Drain valve, (4) Suction filter, (5) Main pump, (6) Pressure filter, 7) Sectional valve, (8) Manometer, (9) Pressure regulator, (10-11) Pesticide tank, (12-13) Feeder pumps, (14-15) Electromotor, (16) Speed signal radar, (17) Central unit.

Target-sensing sprayers, real-time spraying

The observation and recognition of the target plants are basic elements of the target sensing and real-time spraying as well as the quick on-site data processing and the correct pesticide output. The sensing of the target weed may be based on using infrared beam, on wavelength of reflected light, or real image analysis. The multi-sensor system is somewhat more complicated (Fig. 7). In this case plant sensors and solenoid valves will be mounted onto the boom before each of the nozzles. Here there is no real image processing yet, the sensing will be made by photodiodes based on recognition of reflected light of wavelength typical for the target weed.

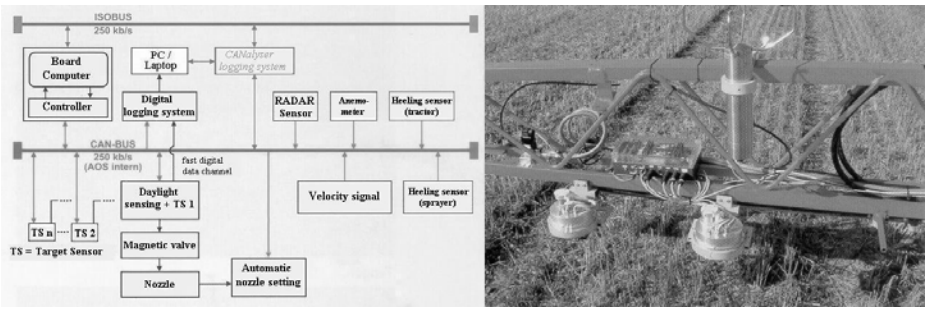

Fig. 7 Schematic overview of the electronic net of the multi-sensor system and individual plant sensors.

To avoid undesired effect of speed differences, a radar-sign will be used. All the sensing and command devices communicate through a special electronic net including the computer, data collector and control monitor, built in the driver's compartment.

The modern spraying techniques are able to give treatments to weedy field spots as small as 15x15 cm. A photo-camera mounted to the head of the machine produces digital pictures of a given field strip and forwards it into the computer of the drivers compartment to process it. A Windows NT-based operational system runs on the computer, producing a weed map for the control panel and communicates continuously with the programmable logic controller (PLC). Ethernet connection exists among the units (Fig. 8). The data processing and command must be quick enough because of the time-delay of the hydraulic system and must be conform with the changing machine speed, too. The PLC unit controls the solenoid valves built just ahead of the nozzles. The nozzles can be switched on/off individually, and they spray onto the weed-infested field spots reproduced on the weed map. In this system there is no previously mixed chemical and water, but during the spraying concentrated fluid pesticide will be injected into the water-flow creating different concentrations as needed. For this an exact liquid measuring is necessary, which will be made by a flow-meter of Raven SCS-700 typ. The computer will determine the amount of op to four different pesticides to be used, depending on the machine speed and severity of weed infestation (Gillis et al., 2003).

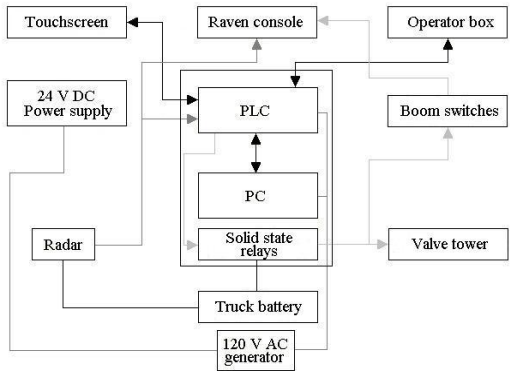

Fig. 8 Schematic overview of the real-time control.

The combined using of different plant sensors and image processing enables working of autonomous sprayers. According to Korean scientists Cho and Ki the machine vision and fuzzy logic determines the working direction of the sprayer, while ultrasound recognizes the plant surfaces (foliage) to be sprayed.

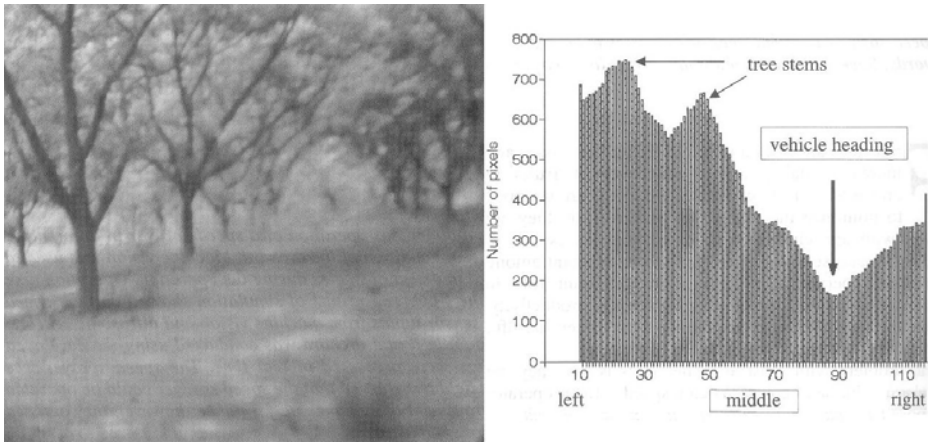

Fig. 9 Machine vision and image processing to determine moving direction of an autonomous sprayer.

For steering and control of a full automatic sprayer the conventional „yes" or „no" or 1 and 0 values are not enough for control, therefore more detailed „real values" by help of fuzzy logic are necessary, like 0,5 („partly"), 0,2 („somewhat"), 0,8 („fairly"). The main components of such an autonomous sprayer are: camera, ultrasound sensors, fuzzy logic controller and hydraulic steering and driving. A black-and-white CCD camera will see the weeds and send digital data in 512x512x8 pixel resolution to an image analyzer software. This camera is mounted to the head of the sprayer. The

forwarded data will be processed in form of 128x128 pixel pictures. After digitalization a histogram will be created from the data (Fig. 9) by which the FLC will determine the optimal driving direction and send a command signal to the hydraulic driving. The data processing takes 1,2 sec using a normal IBM PC 486. Ultrasound sensors mounted in front and up on the machine will measure the distance of the machine from trees and other plants, those mounted to back and side will observe plant leaves and switch off/on the boom sections right and left. The FLC output signals will be interfaced with solenoid valves through an Intel 8255 and the relies used as an i/o interface (Cho, 1999).

Decreasing of pesticide losses

Considerable amount of pesticides can be saved and decrease of environment pollution achieved by speed-related output, using of air-assisted sprayers, controlled droplet applications, target sensing techniques and site specific methods by seriousness of the infection (Fig. 10).

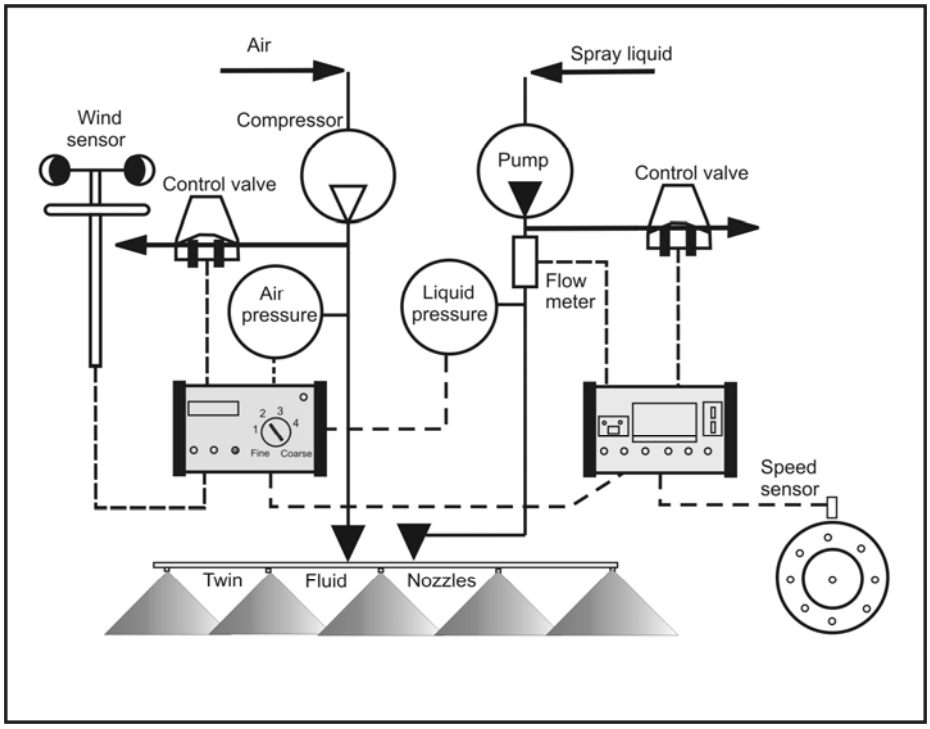

Fig. 10 Model of wind-related droplet production

The advantages of this system are:

- nearly stable droplet size will be achieved in a wide dose and speed spectrum,
- avoids droplet drift into water supplies and neighboring cultures,
- lower liquid use, and by this a larger area can be sprayed.

Air-assisted spraying

In cultures of the arable land this method was successfully used. An air stream pressed above the nozzles transports the droplets onto the

target plants (Fig.11). The amount, speed and direction of the air can be regulated, and this allows spraying even at a wind speed of 5-6 m/s.

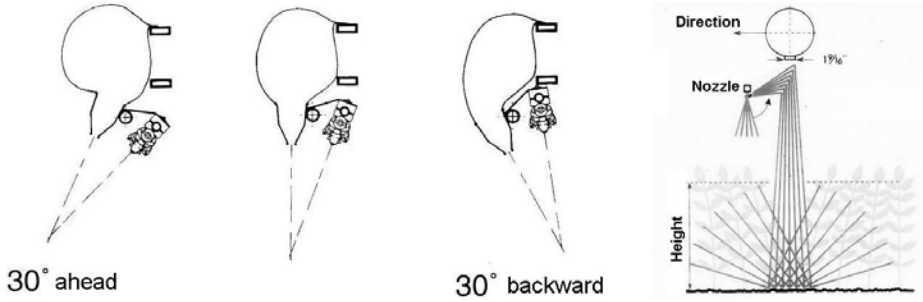

Fig. 11 Air-assisted spraying

Investigations on micro-size distribution of droplets

The effectiveness of spraying is influenced by the droplet size distribution produced by the nozzles. The parameters of the ideal range of droplets (droplet size, droplet number, covering rate, homogeneity, active substance distribution) can be ensured by optimization of the droplet size, and can be measured or estimated by different methods: by direct observation of the spreading, or by sampling.

The direct spreading observation gives distortion free, real and reproducible data. The sensing, measuring and evaluation can be combined into one step if laser technique + electro-optical system + PC will be used together.

At the sampling method color-marked water will be sprayed into silicon oil, and the size of droplets will be evaluated by image analyzer. To measure droplet distribution on the crop leaves, spraying onto water-sensitive paper, film samples or real leaf samples can be used. Determination of droplet characters can be made by PC-assisted image

analyzer, by a covering meter, and the measuring of active substances sprayed onto the leaves by a spectrofluorimeter.

In the last years investigations have been made on hydraulic nozzles, on mechanical rotation nozzles (CDA) and on their covered types, as well as on air injection nozzles and asymmetric nozzles. To determine droplet structure water sensitive paper sampling were made during working the nozzles at different pressure (and rpm) using the following image analyzer system and modules:

- data input for individual droplet structure were made by a SONY CCD monochrome video camera with a Computer TEC-M55 F2,8 objective,
- for measuring at operating the sprayer to determine covering rate, droplet number and active substance distribution a HP ScanJet 6100C scanner of 600 dpi physical resolution was used,
- for communication between the camera and program: Fidelity 200 grabber card,
- for image analysis : GLOBAL LAB Image software,
- for data analysis: Excel programs adjusted to the individual investigations.

The first step of the image analysis is the perception of the droplets on the sampling paper (Fig. 12). The optically magnified picture by the camera will be introduced through a grabber card to the image analyzer program. Since the camera is able to percept just a determined number of pixels, in order to increase the accuracy of the measuring the rate of magnification will be adjusted to the droplet sizes. The pictures recorded by the 600 dpi resolution scanner are sufficient to the desired accuracy, moreover this recording system need a shorter input time. The analysis can be made using a 256 gray-scale picture or using color photo, where to each color an individual gray-scale will be given. Following these transformations the yellow background of the samples differs well from the darker spots of the droplets. Segmented and detected the pictures they are ready for measurements. Some steps of the preparation are shown on Fig. 13 Following these transformations the yellow background of the samples differs well from the darker spots of the droplets..

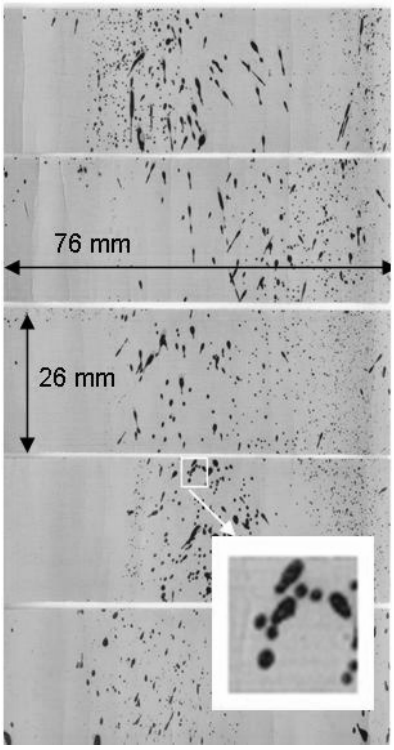

Fig. 12 Water sensitive paper sample used at investigation of a TX ConeJet VK 26 type nozzle at work.

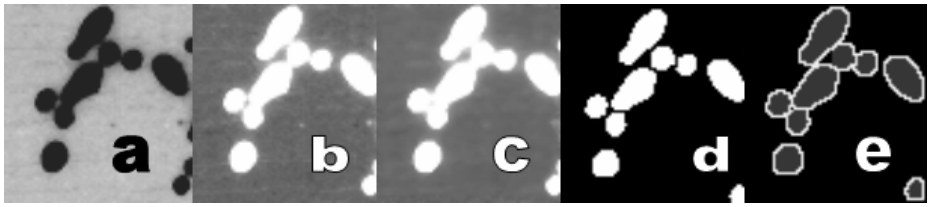

Fig. 13 (a) color to gray transformation, (b) inverse picture (easier to follow visually), (c) noise reduction, (d) detection and watershed, (e) transformation.

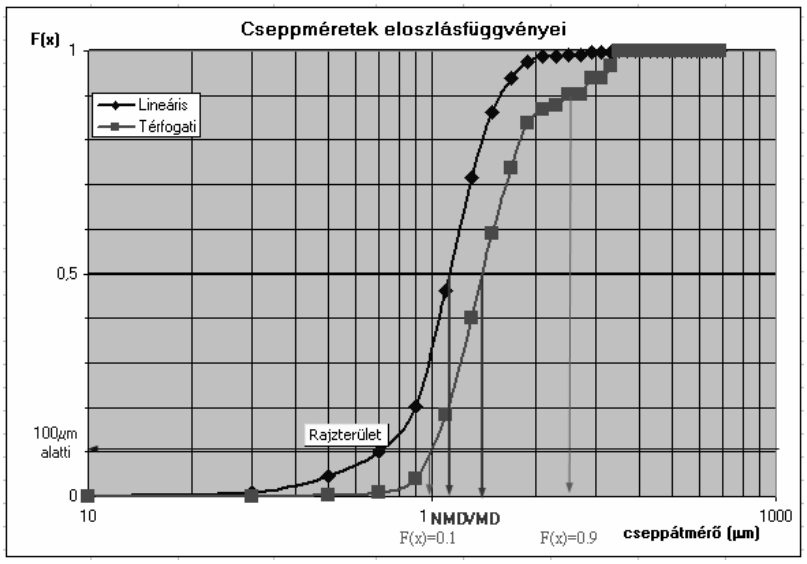

Fig. 14 Droplet structure by a rotation nozzle of type Micron X1 at rpm n=1410 1/min.

After calibration the data transformed will be evaluated by using an Excel program adjusted to the method of investigation. From the area of the flattened droplets their diameter are counted, then their density function represented according to their size and also their cumulative frequency are represented on logarithmic diagrams based

on their size and volume. The diagram on Fig. 14 shows the most important characters of the pulverization.

Conclusions

The improvement of new techniques and the development of technical procedures are essential for an increasing effectiveness and safety in the plant protection. These can also considerably decrease the losses and ensure a better and more uniform covering of the plants ith pesticides. Utilizing the modern informatics it became possible the usage of wind-related spraying with regulated droplet size, the air-assisted spraying, the target-sensing spraying, the site-specific and by the seriousness of infection the regulated spraying.

Using a special operation, by which active injectors can press air into the nozzles, wind-relating droplet-producing system was developed. In this system a computer determines the droplet size based on wind-speed measuring, to avoid droplet drift. For this the computer gives command to regulate the pressure of the liquid and the assisting air. The amount of pesticide mixture can be reduced to 100-200 l/ha, and a safe spraying can be made even at a wind speed of 4-5 m/s. In case of the air-assisted spraying an air stream will be blown out of a tube located above the nozzle and this transports the pesticide droplets onto the target surface. The speed, amount and direction of the air stream are well regulated allowing the spraying even at a wind speed of 5-6 m/s.

More solution has been developed for the site-specific treatment. The orchard sprayers provided with infrared or ultrasonic

plant sensors switch off the nozzles in lack of tree leaves, which means, that spraying happens in the presence of leaves only. Using GPS a weed map can be produced and the spraying can be directed by using the map. The site-specific spraying can be made also by help of direct observation of the weeds using for this cameras or other sensors. The automated differentiation of cultured plants and weeds allows pesticide output according to the severity of the infestation. For this nozzles with different outlet openings can be mounted onto the boom, to switch on/off the openings individually or together according to the infection rate, to spray out different amounts of pesticide mixture.

References

Cho, S.I., Ki, N.H. 1999: Autonomous Speed Sprayer Guidance Using Machine Vision and Fuzzy Logic, Transactions of the ASAE, 4, 1137-1143.

Csizmazia, Z. 2006: A növényvédelem gépei (Machines of plant protection), Mezőgazda Kiadó, Budapest, p:114.

Gillis, K.P., Giles, D.K.,Slaughter, D.C., Downey, D. 2003: Injection Mixing System for Boomless Target-Activated Herbicide Spraying, Transactions of the ASAE, 4, 997-1008.

László, A., Pályi, B., Mátrai, Z.: Precíziós (szabályozott, helyspecifikus) növényvédelmi kijuttatástechnika (Precision spraying in plant protection). XL. Georgikon Napok Keszthely, 1998. 09. 24.-25., Különkiadvány III. köt., 267.-271.

Martina Koller, M., Lanini, W. T. 2005: Site-specific herbicide applications based onweed maps provide effective control, California Agriculture 3, 182-187.

Pályi, B., László, A., Rietz, S., Ganzelmeier, H. 2006: Comparison of Electronic Control Units for Field Sprayers. Georgicon for Agriculture, Keszthely 16 (1), 55-75.

MODELLING AND IDENTIFICATION OF SOLAR COLLECTORS WITH COMPUTER SIMULATION

Botond Cseke*, Béla Pályi

University of Pannonia, Georgikon Faculty, H-8360 16 Deák Ferenc Street Keszthely, Hungary. E-mail: cseke@georgikon.hu

Abstract

To design a solar thermal system with solar collectors, it is important to be able to define the amount of heat provided by solar collectors. The heat produced depends on the construction parameters of the collector and the entire system the characteristics of the operation and the climatic conditions of the installation site. The available basic calculation methods for sizing solar thermal systems are only suitable to preliminary estimations, in most cases accurate sizing is usually carried out with computer-assisted modelling. To develop a model for a solar thermal system first the model of the solar collector was developed. To simulate the Viessmann Vitosol 200 D30 vacuum tube collector the Hottel-Vhillier model was used. The solution of the equation provided by the model and its validation with measured data was carried out by the block-oriented Matlab+Simulink software package.

Keywords: renewable energy, solar energy utilisation, vacuum tube collector, thermic simulation, Hottel-Vhillier model, Matlab and Simulink software.

Összefoglalás

A napkollektoros hőtermelő rendszerek tervezésénél fontos a kollektorok által termelhető hőmennyiség meghatározása. A termelt hő függ a kollektor és a rendszer konstrukciós paramétereitől, az üzemeltetés jellemzőitől ill. a telepítés helyszínének klimatikus jellemzőitől. A rendszer méretezéséhez rendelkezésre álló alapösszefüggések csak előzetes becslésre alkalmasak, pontosabb méretezés számítógépes modellezéssel végezhető. A rendszer termikus modellezésének szerves része a kollektor modellezése. A Viessmann Vitosol 200 D30 vákuumcsöves kollektor szimulációjához a Hottel-Vhillier modellt alkalmaztuk. A modell által szolgáltatott egyenlet megoldását ill. mérési adatokkal történő ellenőrzését a blokkorientált Matlab+Simulink programcsomag segítette.

1. Introduction

Prior to the installation of solar collector operated heat utilisation systems, it is possible to define the performance of the system by modelling it with the demands, local characteristics and the technical parameters of the equipment devised. For the simulation of the operation of the system, it is inevitable to make physical models of the different components (collector, heat exchanger, storage unit) which describe their energy balance (relations). The solutions of the

equations and the validation of the developed models based on measured data are well supported by the Matlab+Simulink block-oriented software package. As the result of the computer simulation, it is possible to define the parameters of the equipment's performance, the collector surface and the heat storage capacity. (Buzás et al., 2000.) Since the 1990s Farkas and his colleagues have been working on the block oriented modelling of several solar collector equipment. Taking the data of several one-day-long periods as a basis, they made the full model of a flat plate solar collector system and then with backfeeding the measured data of the model they found that the system lends itself to modelling by using physical models. At our department, we carried out the block oriented modelling of a vacuum tube solar collector based on the technical specification of the operating collector, using the measured data acquisited during a whole calendar year.

2. Materials and methods

2.1. Description of the solar collector and the tested solar thermal system

It was in January 2004 at the Department of Agricultural Mechanisation of the Georgikon Faculty of Agriculture (the University of Pannonia) when a vacuum tube solar collector hot water system was installed both to serve scientific and educational purposes and to meet the hot water demands of the training workshop. The system has two collector loops side by side, both of which work for a 500 litre hot water storage tank (Fig. 1). For one of the collector loops there were 3 selective flat plate collectors installed each with a useful area of

1.76 m^2, while for the other collector loop a 3 m^2 vacuum tube collector was installed (type: Viessmann Vitosol 200 D30; for technical characteristics see Table 1.; for construction see Figure 2.) to serve heat generation. The collector-units are south-oriented, with tilt angles of 33°. The two loops have independent/separate circulation pumps, installed in the collector return pipes, controlled by two separate controllers.

The monitoring of the solar thermal system heat production is supported by a HC-23 type, microprocessor based data collecting unit, which automatically picks data from the measured points at regular intervals of time set. The data stored at each measurement tome and point: solar irradiation intensity, outer ambient temperature; for each collector loop: the temperature entering and re-entering the collector, the mass flow, the water temperature of the inlet and the outlet and also taken at three different altitude points and the quantity of the hot water used. Data are picked at every 5 minutes (customised) besides this, at every change of the system's conditions, the data collector picks the respective data, all the data are transmitted to the port of the PC taking the registration and then a software continuously run on DOS, saves the data in table format. The data acquisition system is suitable for continuous data registration, saving the data in newer and newer files every oncoming month.

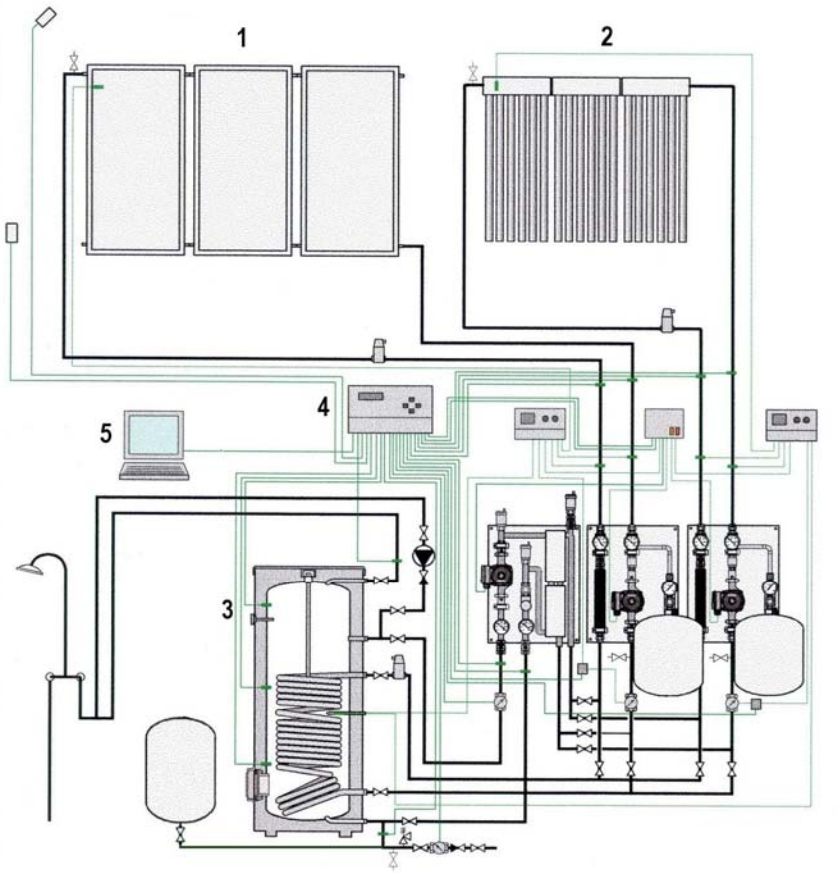

1. flat plate collectors; 2. vacuum tube collectors; 3. hot water tank;
4. HC-23 microprocessor based data acquisition system; 5. computer

Figure 1: The sketch of the solar thermal system

2.2. The mathematical model of the solar collector

The main question of modelling solar collectors is how to find the best possible, most usable model. In practical cases, especially in agricultural applications it is satisfactory to use a les sophisticated dynamic model. It is often enough to calculate the temperatures of the heat transfer fluid all along the full length of the collector (Farkas 1999.)

Type		D30
Number of tubes		30
Gross area	m^2	4.38
Absorber area	m^2	3
Aperture area	m^2	3.21
Dimension		
Width	mm	2159
Height	mm	2028
Depth	mm	138
Optical efficiency	%	84
Heat loss correction value K1	$W/(m^2*K)$	1.75
Heat loss correction value K2	$W/(m^2*K)$	0.008
Weight	kg	68
Heat transfer medium content	litre	6
Permissible operating pressure	bar	6
Max stagnation temperature	°C	300
Connections	Ø mm	22
Required installation area on flat roofs	m^2	4.38

Table 1: Technical parameters of the Viessmann Vitosol 200 D30 vacuum tube collector

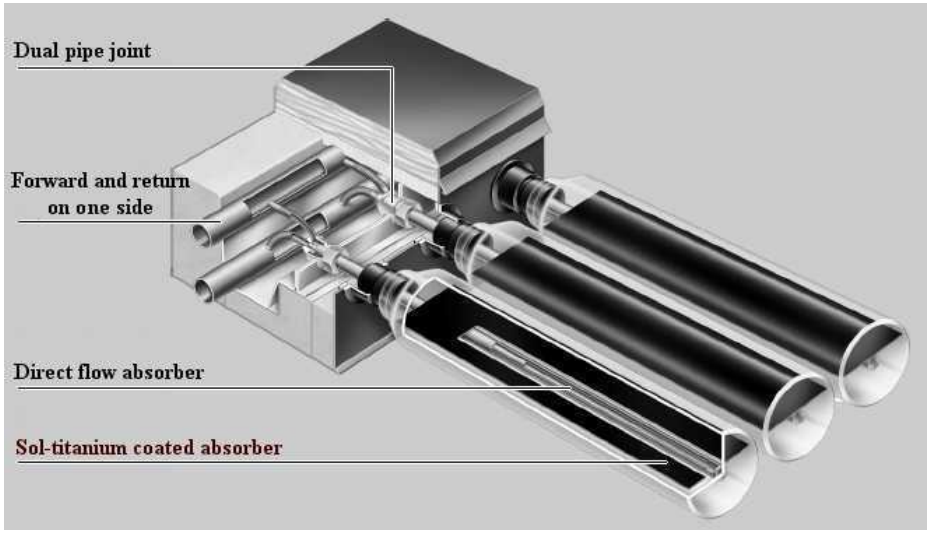

Figure 2.: Structure of the Viessmann Vitosol 200 D30 vacuum tube collector

For the simulation of the collectors tested we used the Hottel-Vhillier model. It gives the temperature distribution of the flowing heat transfer fluid as a function of time and place. The equation to describe it is as follows (Farkas 1999.):

$$T(x,t) = T_W(t) + \frac{I(t)}{k_{aw}} + \left[T_{in}(t) - T_W(t) - \frac{I(t)}{k_{aw}} \right] \cdot e^{\frac{-k_{mw} \cdot w \cdot x}{c_m \cdot \dot{m}}}$$

where :

c_m specific heat of the heat transfer fluid [J/kgK]

T_w ambient temperature [°C]

I solar irradiation intensity [W/m^2]

x length of the collector [m]

$\dot{m}$ mass flow rate [kg/s]

w width of the collector [m]

T the collector's outgoing temp [°C]

t time [s]

T_{in} inlet collector temperature [°C]

k_{aw} heat transfer coefficient between the absorber and the environment [W/m^2K]

k_{mw} heat transfer coefficient between the heat transfer fluid and the environment [W/m^2K]

The above model gives the temperature of the heat transfer fluid along the length of the collector. The identification of the heat transfer parameters (k_{aw} and k_{mw}) can be made based on measured or calculated data. The parameter identification problem can be defined by minimization of the difference between the calculated (c) and the measured (m) temperature in the given time period (t). Carried out the identification the least square method was used as an objective function (Buzás 2005):

$$J[k_{aw}, k_{mw}] = \int_{t_0}^{t_e} \left(T_c(t) - T_m(t)\right)^2 dt \Rightarrow MIN$$

2.3. The data system used for simulation and the Simulink model

We used measured data of the period ranging from 1 April 2004 to 31 March 2005 to simulate the outlet temperature of the tested collector. The columns of the data matrix were: time of measurements [s], irradiation-intensity [W/m^2], ambient temperature [°C], temperature of the heat transfer fluid entering the collector [°C], temperature of the heat transfer fluid leaving the collector [°C].

From the data matrix above we deleted the sets of values belonging to the switched-off state of the circulation pump. (e.g. at night and when it was overcast), as well as at the beginning and at the end of operating periods, when there were some minutes with unstable (unreliable) operation. These periods are characterised by the alternation of the pump's switched off/on conditions, which significantly influences the evenness of heat transfer, that is it would produce data rendering the simulation unreliable. The measured data matrix (M matrix) acquired this way was saved in database for the Matlab programme.

The Hottel-Vhillier model's block oriented solution was used for the simulation (Fig. 3), which can be created with the Simulink software as a toolbox of to the Matlab (Buzás 2005).

The assumptions taken into consideration at the application of the model can be summarised as:

1. During the operation period, the specific heat and density of the heat transfer fluid (1:1 mixture of water and propylene-glycol) is considered constant;

2. The mass flow of the heat transfer fluid is considered constant all through the circulation;
3. The heat capacity of the individual components of the collector tested is ignored;
4. All the elements of the active surface of the collector tested is considered as having the same temperature;
5. Examining any cross-section of the absorber tube, we take the conditions of heat transfer as being the same;
6. The pipe-in-pipe absorber of the vacuum tube collector is considered as a simple absorber pipe in the simulation;
7. The active width of the vacuum tube collector unit is the sum of the widths of the absorber strings to be found in the pipes.

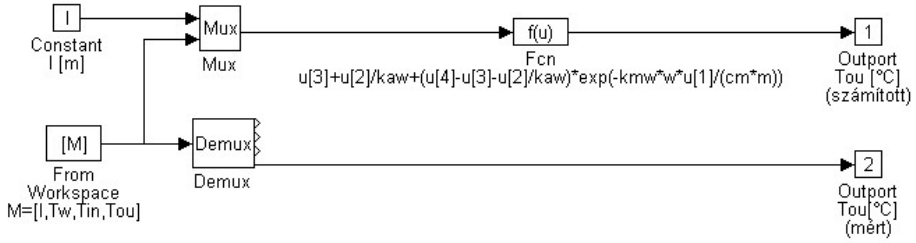

Figure 3: The model of the solar collector in Simulink

3. Results

3.1. Steps and result of the simulation

First we ran the Matlab programme's *kollvak.m* file, which contains the *M* measured datamatrix and the values of the model parameters. Then we defined the k_{aw} and k_{mw} parameters as being global variables and gave them the starting value 1.

Then giving the time period, we had the simulation carried out by using the Simulink model. The program calculated the results given in Fig. 4.

The horizontal axis displays the time, in second, while the vertical axis gives the collector outlet temperature in °C. The two curves we got show the measured (continual line) and the calculated (broken line) values respectively. Fig. 4 shows that when k_{aw}=1 and k_{mw}=1 in the best part of the test period, the outlet collector temperature values calculated by the model are far cry from the measured values.

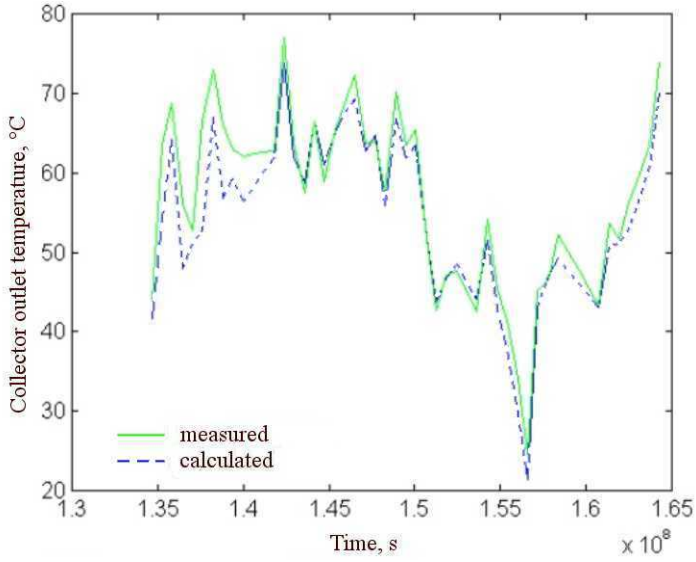

Figure 4: Collector outlet temperature before parameter identification, when $k_{aw}=k_{mw}=1$

The next step was the parameter identification, that is finding values for k_{aw} and k_{mw} with which the Hottel-Vhiller equation approximates the outlet collector temperature values based on measured ones with the least possible error within the test period. It needs running the *kidvak.m* file (used for the identification) which

contains the time when measurements were taken and the corresponding measured outlet collector temperatures; gives commands to have the above simulation run again and then calculates the differences and the square sum of the measured and calculated outlet collector temperatures with the respective k_{aw} and k_{mw} values. First we defined the parameters to be identified in the Matlab command window as being global variables. We had the *kidvak.m* file run as a trial with 1;1 values and then with 10;10 values just to make sure the parameter transfer works. Then we started the Matlab built in minimization algorithm the result of which was the parameters wanted: k_{aw}=8.5022 k_{mw}=24.1497

Finally after running the Simulink model with the parameters identified, and the results displayed, we got the curve to be seen in Fig. 5.

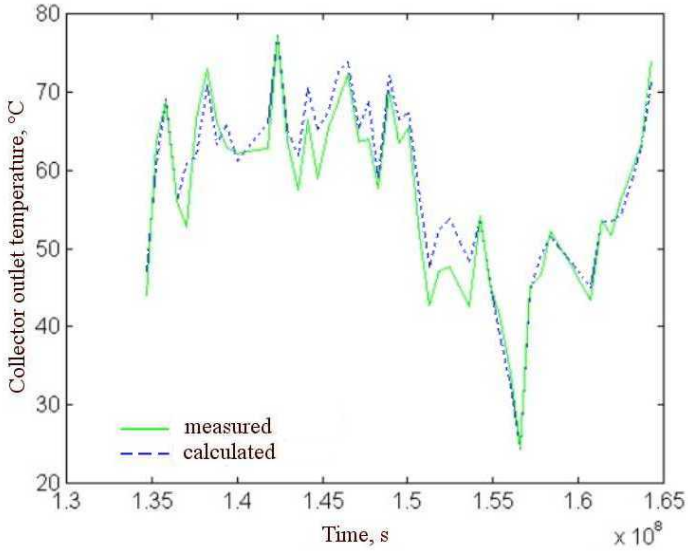

Figure 5: Collector outlet temperature values after parameter identification

3.2. Model validation – comparison of calculated values with a set of measured values

The parameters k_{aw} and k_{mw} identified in the way described above, are to be placed back in the Hottel-Vhillier equation and it gives the equation describing the tested collector model, which - using the starting data – calculates the temperature of the heat transfer fluid leaving the collector. Naturally, the model is suitable for giving approximate calculations, the exact outlet temperature can only be defined with measurement. The validity (goodness) of the model can only be evaluated if it is compared with the 'outlet heat transfer fluid temperature' column of a measured data matrix. Here we are to use the data matrix of a period of time other than that used at the identification of the model.

To check the model we used the data matrix of June 2005. The comparison of the measured and calculated values was made in an Excel table. The data matrix contained 502 measured samples. The maximum deviation of the model from the values measured was 12.05 °C, the average deviation within the measured period was 1.74 °C.

Discussion

The deviation averages to be reached by the model are within 2 °C, which - in case of a simulation based on the data matrix of a whole year - is satisfactory. In some cases there were 10-12 °C differences from the actual temperatures. The reason is might that the model does not take into account the heat capacity of the collector elements and the resulting slow reaction to the changes of the environment parameters.

The temporarily unstable data of the starting and before-finish periods were ruled out, however, in the data-line there must be some data that registered changes beyond the sensitivity of the model such as e.g. a sudden cloudy period made the model register the actual decrease of the irradiation-intensity, while the temperature of the heat transfer fluid leaving the collector still showed higher values corresponding to the previous high irradiation-intensity. The simple model is not able to exactly simulate such events, which might give rise to occasional higher error values.

Taking the magnitude of the average deviation into consideration we can state that the collector model is suitable to give approximate calculations to estimate the outlet temperature of the heat transfer fluid. As the given model is capable of simulating the normal operation of the solar collector with a good approximation, it can be declared that using the calculated outlet temperatures, it is suitable to provide approximate calculations for the possible heat production.

Acknowledgement

Hereby we would like to express our gratitude to Prof. I. Farkas and Mr. J. Buzás (Department of Physics and Process Control, Szent István University), who providing ample consulting opportunities and helpful criticism greatly contributed to the growth of theoretical knowledge about computer assisted simulation as well as its practical realisation.

References

Buzás, J. , Farkas, I., Biró, A., Németh, R., 1998. Modelling and simulation aspects of a solar hot water system. *Mathematics and Computers in Simulation*, **1.** 33-46.

Buzás, J., Farkas, I., 2000. Block oriented modelling of solar domestic hot water system, *Mezőgazdasági Technika*, **5.** 2-3. (in Hungarian)

Buzás, J. 2005. Educational supplement to Computer simulation. University course book; Solar collector models with Simulink software, Faculty of Mechanical Engineering, Szent István University (in Hungarian)

Farkas, I. 1999. Computer assisted simulation. University course book; Faculty of Mechanical Engineering, Szent István University (in Hungarian)

Farkas, I., Buzás, J., Lágymányosi A. 2000. Data acuisition system for a solar domestic hot water system installed on a family house, Report, Department of Physics and Process Control, Szent István University, No. 18, Gödöllő, October 2000 (in Hungarian)

Farkas, I. 2005. Process control. University course book; Faculty of Mechanical Engineering, Szent István University (in Hungarian)

Merényi, L. 2000. TRNSYS simulation model of a solar domestic hot water system. 6th Workshop on Energy and Environment, Gödöllő, Hungary.

Seres, E., Farkas, I., Biró, A., Buzás, J., Lágymányosi, A. 1997. Data logging and monitoring tools used for simulation and modelling of a solar system, Proceedings of IMACS/IFAC Second International Symposium on Mathematical Modelling and Simulation in Agriculture and Bio-Industries, May 7-9, 1997, Budapest, Hungary, 277-282.

OBSERVATIONS AND TUMOUR INCIDENCE OF CONTROL CRL:CD BR RATS IN A 2-YEAR CARCINOGENICITY STUDY BY NORMAL CALORIC INTAKE

István Sebestyén*, László Várnagy, Péter Budai

University of Pannonia, Georgikon Faculty of Agriculture

Institute of Plant Protection Department of Hygiene

16 Deák F. Street Keszthely,

istvan.sebestyen@mailbox.hu

Summary

The pesticides and other chemicals used during the agricultural production mean hazard for either the plants or animals, and through the food-chain or during the work for peoples. So the stipulation of use and circulation of these chemicals is authority registration. The organic part of the registration documentation is the data of animal experiments including the 2-year carcinogenicity study on rats or mice, which is necessary for the final permission. On the basis of this study the potential carcinogenic effect of the chemical product can be estimated during a long-term, even life-span repeated exposition.

This assay summarize the results of observations and incidence of spontaneous tumours of the control groups of a 2-year

carcinogenicity study in Crl:CD Br rats with normal caloric intake. In the control group of the study 50 animals of both genders were used. Animals were observed for 104 weeks, particular attention was paid to observe the tumour development during the palpation examination. The body weight and food consumption of animals were regularly measured. The body weight gain, and the daily food consumption per animals were calculated. Haematological investigations were performed by blood smear evaluation at 12th, 18th and 24th months. At termination detailed necropsy was performed and the weight of selected organs was measured. All organs and tissues fixed were subjected to histopathological examinations. At histopathological evaluations the observed neoplastic and non-neoplastic alterations were identified and their frequency was evaluated.

The effect of *ad libitum* feeding manifested in the fast body weight gain in the first year of the study. We observed slightly increased mortality of male rats at around the 18th month of the study, which can be in connection with the rapid body weight gain of young male animals. In spite of the *ad libitum* feeding, the percent survival of both sexes was above 50% at the end of 24th month, which is the important acceptance criterion of the carcinogenicity studies. The haematological findings and organ weight data well demonstrated the age-related changes of the parameters of experimental animals. On the basis of the pathological and histopathological results the most common causes of death observed during the study were the pituitary adenoma, which is common in the rat strain observed, malignant (often

generalized) tumours, chronic nephropathy, lung oedema and serious cystic degeneration of the adrenal glands.

Our results can be used as historical control data during the evaluation of carcinogenicity studies performed in the investigated rat strain under similar conditions.

Keywords: toxicology, authorisation, carcinogenicity study, rats, feeding, historical control

Összefoglalás

A mezőgazdasági termelés során felhasznált növényvédő szerek és egyéb kémiai anyagok veszélyt jelentenek mind a kezelt növényekre, az állatvilágra, mind a táplálékláncon keresztül vagy a munkavégzés során az emberekre. Az anyagok felhasználása és forgalmazása hatósági engedélyhez kötött. A regisztrációs dokumentáció szerves részét képezik az állatkísérleti adatok, beleértve a két éves karcinogenitási vizsgálatokat patkányokon és egereken, amelyek szükségesek a végleges engedély megadásához. Ezen vizsgálatok alapján a kémiai termékek hosszú távú, akár élethosszig tartó expozíciójának potenciális daganatkeltő hatása megbecsülhető.

Jelen munkánk összefoglalja egy Crl:CD Br patkánytörzsön szokványos kalória bevitel mellett végzett kétéves karcinogenitási vizsgálat kontroll csoportjának megfigyelési eredményeit, valamint az észlelt spontán daganatok gyakoriságát. Nemenként 50 állatot alkalmaztunk a kísérlet kontroll csoportjaként. A kísérleti állatokat 104

héten át megfigyeltük, különös gondot fordítva a daganatok fejlődésének megfigyelésére a palpációs vizsgálatok során. Az állatok testtömegét és tápfogyasztását rendszeresen mértük. A testtömeg gyarapodást és a napi, állatonkénti tápfogyasztást kiszámoltuk. A kísérlet 12., 18. és 24. hónapjában hematológiai vizsgálatokat végeztünk vérkenet értékeléssel. A kísérlet végén részletes kórboncolást végeztünk, és a kiválasztott szervek tömegét megmértük. Minden tartósított szervet és szövetet szövettani vizsgálatnak vetettünk alá. A szövettani vizsgálatok során azonosítottuk a megfigyelt daganatos és nem-daganat eredetű elváltozásokat, illetve értékeltük ezen elváltozások gyakoriságát.

Az *ad libitum* takarmányozás hatása a gyors testtömeg gyarapodásban jelentkezett a kísérlet első évében. Kissé magasabb elhullási arányt tapasztaltunk a hím állatoknál a kísérlet 18. hónapja körül, ami kapcsolatban lehet a fiatal hím állatok nagyon gyors testtömeg gyarapodásával. Az *ad libitum* takarmányozás ellenére a túlélés százalékos aránya a 24. hónap végén 50% felett volt mindkét nemben, ami a karcinogenitási vizsgálat fontos érvényességi kritériuma. A hematológiai leletek és a szervtömeg adatok jól mutatják a kísérleti állatok paramétereinek korral összefüggő változásait. A kórbonctani és szövettani vizsgálatok eredményei alapján az elhullások leggyakoribb oka a hipofízis daganat volt, ami jellemző a megfigyelt patkánytörzsre, valamint a rosszindulatú, gyakran generalizált daganatok, krónikus vese elfajulás, tüdő ödéma és a mellékvese savós cisztás degenerációja. Eredményeink történeti kontrol adatbázisként

használhatók hasonló körülmények között az említett patkánytörzsön elvégzett karcinogenitási vizsgálatok értékelése során.

Introduction

The pesticides and other chemicals used during the agricultural production mean hazard for either the plants or animals, and through the food-chain or during the work for peoples. The determination of the risk or hazard represented by the chemical product is performed by the toxicology, as interdisciplinar science. One of the main fields of the usage of toxicological data obtained during the in vivo or in vitro toxicological studies is the authority registration for using and circulation of the pesticides and other agricultural chemicals. In case of pesticides, The Plant Protection Products Directive (91/414/EEC), 'The Authorisations Directive', was adopted by the Council of Ministers on 15 July 1991 and is implemented in Hungary by the Plant Protection Law, 2000. XXXV., and the regulation 89/2004. (15 May FVM) and (EC, 1991; EC, 1997), contain the data requirements and procedures for pesticide registrations. The organic part of the registration documentation is the data of animal experiments including the 2-year carcinogenicity study on rats or mice, which is necessary for the final permission. On the basis of this study the potential carcinogenic effect of the chemical product can be estimated during a long-term, even life-span repeated exposition (Wallace, 1989).

The most important symptom in the carcinogenicity studies is the tumour (benign or malign) and the decision is very important if the

tumour developed spontaneously, which is age-dependent process in the rodents, or induced by the exposition to the test item. The presence and evaluation of the historical control data is also very important during the evaluation of the carcinogenicity study in dividing the spontaneous and the treatment-related tumours and expressing an opinion about the test item, which is the basis of the risk assessment during the registration procedure and releasing for trading (Tannenbaum, 1959; Ross et al, 1971; Kritchevsky et al, 1989).

The objective of the carcinogenicity studies are to observe test animals for a major portion of their life span for the development of neoplastic lesions, as part of a program of animal toxicity experiments designed to provide information which will allow the test material to be safe for a long-term use. The acceptable methods of carcinogenicity studies are described in international standards (OECD, 1981; EC, 1988; US EPA, 1988; FDA, 1996).

This assay summarize the observations, incidence of spontaneous tumours of the control groups of a carcinogenicity study in Crl:CD Br rats. The control group of this study received „normal" diet which allows the normal caloric intake usual in short-term studies. Caloric intakes are now recognized to be important uncontrolled variables in bioassays because rodents chronically fed *ad libitum* become obese, reproductively senile and have increased incidences of age-related diseases, higher tumour burdens and decreased survival (Garfinkel, 1985; Lyon et al, 1987). Already in 1975 Berg suggested that it might be pertinent to correlate tumour risk with overall dietary life-style.

Our results can verify the latter assumptions and can be used as historical control data during the evaluation of carcinogenicity studies performed in the investigated rat strain.

Materials and Methods

Experimental animals

Crl:CD Br (Sprague-Dawley) rats were used in this study. The source of animals was the CHARLES RIVER WIGA GmbH, Sandhofer Weg 7, D-97633 Sulzfeld.

The rat is an internationally accepted species for carcinogenicity studies. The Crl:CD Br rat is widely used for this purpose, therefore historical data are available.

The study was started with 50 male and 50 female animals / groups. The age of animals at reception was 5 - 6 weeks. The quarantine and acclimatization period was 14 days after the reception of animals. The body weight range of male animals was 120-148 g and the female animals was 112-131 g at reception.

Hygiene and Health Conditions

The studies were started with animals of SPF state (certified by supplier).

The animals were maintained behind a specified barrier system, in separated room equipped with sterile air-conditioning system, air filtered by bacterial filter EU9.

The animal unit had a clean corridor separated from a dirty corridor by a barrier system with personnel and material lock.

Cages and bedding were changed as required. Water bottles were cleaned on a rota basis as required during the course of the study.

Room sanitation: the floor was swept and then mopped with an acceptable disinfectant at the end of each working day.

Only animals in acceptable health condition were used in the study. The health condition was certified by the responsible veterinarian on the basis of external clinical examination and the results of base level examinations.

Husbandry

Group caging was used at the beginning of this study, 5 animals were housed per cages at start of examination, 3 animals/cage from the 6th month and individual caging was used from the end of the first year. Animals were housed in Techniplast T III plastic cages. Certified laboratory bedding was used during the study. The microbial state of each batch of bedding was checked. 12 hours lighting was supplied daily from 6 am to 6 pm.

The range of room temperature was 22 ± 3 °C, the relative humidity 50 ± 20 %. Air changes were 10-15 changes per hour, pressurized.

The cages were replaced to the place of the next cage as a circulation in every two weeks during the study. The temperature and humidity were monitored regularly.

Food and Feeding

In this study the animals received SSNIFF R/M-Z+H 15 MM AUTOKLAVABLE COMPLET DIET FOR RATS AND MICE - BREEDING + MAINTENANCE. In the assay this diet was called as Normal Diet.

The diet was produced by Ssniff Spezialdiäten GmbH, D-59494 South Germany. The food was offered *ad libitum*. Before the terminal necropsy animals were without food for a night.

The check of ingredients and analytical examinations of diet were done simultaneously. Besides, the diet was analyzed for possible contamination (aflatoxin, pesticide residue, heavy metals) and microbiological sampling was also made from every batch of mixing. Quality control of diet was performed by National Institute for Agricultural Quality Control (42 Remény Str. Budapest Hungary).

Table 1 Nominal Contents of the Normal Diet

Content	Value	Unit of Measure
Crude protein	19.00	%
Crude fat	3.50	%
Crude fiber	4.90	%
Crude ash	6.00	%
AMINO ACIDS		
Lysine	1.10	%
Methionine	0.60	%
Cysteine	0.25	%
Glycine	0.90	%
Leucine	1.50	%
Isoleucine	0.90	%
Arginine	1.20	%
Phenylalanine	0.90	%
Tryptophan	0.25	%
Histidine	0.45	%
Alanine	0.70	%
Tyrosine	0.60	%
Asparic acid	1.40	%
Glutamic acid	2.20	%
Valine	0.90	%

Content	Value	Unit of Measure
TRACE ELEMENTS (per kg)		
Manganese	75.0	mg/kg
Copper	12.0	mg/kg
Zinc	70.0	mg/kg
Iodine	1.5	mg/kg
Iron	220.0	mg/kg
Calcium	1.00	%
Sodium	0.20	%
Magnesium	0.20	%
Phosphorus	0.80	%
VITAMINS (per kg)		
A	27000	IU
D_3	1920	IU
E	180	mg/kg
C	500	mg/kg
B_1	24	mg/kg
B_2	45	mg/kg
B_6	25	mg/kg
B_{12}	90	µg/kg
Biotin	400	µg/kg
Pantothenic acid	60	µg/kg
Choline	2400	mg/kg
Folic acid	6	mg/kg
Nicotinic acid	90	mg/kg
K_3	4	mg/kg
Inositol	60	mg/kg
ME (per kg)	12.3	MJ

Water Supply

The animals received filtered tap water, as for human consumption *ad libitum* from 500 ml bottles (water was filtered by bacterial filter). Quality control of water was performed in every three months by Central Laboratory of Water and Canalization Company of the Capital (23-27 Váci Str. Budapest Hungary). The food and water used was not considered to contain any additional item in sufficient concentrations to have a deleterious influence on the outcome of the study.

Identification of Animals

The individual identification was performed by ear tags or tattooing the tail of the rats. The numbers were given as following:

	MALES	FEMALES
Control	X001-X050	X051-X100

The cages were identified by identity cards, with information about study code, sex, dose group, cage number and individual animal numbers.

Observations

Clinical observations

A careful clinical examination was made and recorded once prior to the initiation of treatment and once weekly during treatment in all animals. Individual observations included the check of the appearance, condition, behaviour, activity, excretory functions, respiration, orifices and eyes. All animals were observed daily to detect onset and progression of all toxic effects as well as to minimise loss due to diseases, autolysis, or cannibalism. Special attention was paid to

tumour development: the time of onset, location, dimension, appearance and progression of each grossly visible or palpable tumour were recorded monthly from the start to 6 month, in every fortnight between 7 and 12 months and weekly thereafter. Animals were examined twice each day for being moribund state and mortality. The date of death was recorded. Animals found moribund were isolated and/or sacrificed. They were processed in the same way as the animals of the terminal necropsy.

Body Weight

Body weight of all experimental animals was weighed weekly during the first 12 weeks of the study and once in every four weeks thereafter with precision of 1 g.

Food Consumption

The quantity of food consumed by the animals of each cage was weighed weekly during the first 13 weeks of study and bi-weekly thereafter with precision of 1 g.

Haematology

Blood samplings were carried out at 12th and 18th months, then at the end of the study from the root of the tongue of every experimental animal. The tongue was pricked with an injection needle and blood was collected by a capillary containing heparin. Blood smear were made taking out the blood from the capillary and the smears were stained by Pappenheim, modified Pappenheim method. In these sampling times differential white blood (WBC) cell count was determined.

Necropsy

From the afternoon of the day before the necropsy the animals were fasted during 16-18 hours before the necropsy. Next day the animals were euthanized by intraperitoneal injection of Nembutal. Thorough post-mortem examinations were performed under the guidance of a qualified pathologist on all animals including those found dead. After the examination of the external appearance the cranial, thoracic and visceral cavities were opened and the appearance of the tissues and organs were observed, any abnormality was recorded with details of the location, colour, shape and size. Selected organs (Brain, Liver, Spleen) were weighted and recorded from all surviving animals at terminal sacrifice with precision of 0.01 g. Relative organ weights were calculated referring to the body weight and brain weight.

Histopathology

During the necropsy all organs and tissue samples of experimental animals were removed for histological examination and preserved in 10 % buffered formaldehyde solution from all surviving animals, moribund killed and deceased. Histological preparations and histopathological examinations were performed on the preserved organs or tissues mentioned above from all animals of the evaluated groups. All grossly visible tumours or lesions were examined and the results were recorded in all groups. The required samples were embedded in paraffin wax and sections cut at approximately 5 microns thick and stained with haematoxylin and eosin. Bones were decalcified in 10 % formic acid. Used literature during the evaluation work were as follows: Growing, 1980; Kardeván, 1976; Papolcsy, 1975; Resnik et al, 1983.

Results

Clinical Observations and Mortality

The proper conduct of carcinogenicity studies is an important part in the evaluation and prediction of potential human carcinogens. Significant reductions in the number of animals surviving to termination have been widely reported in the scientific literature. This is a matter of concern since inadequate carcinogenicity studies could result in studies being rejected, and hence large numbers of animals being needlessly used, or in the failure to identify potential human carcinogens. For a negative result from a rat carcinogenicity bioassay to be considered acceptable, survival at 24 months should be 50% or greater in all groups (OECD, 1981; EPA, 1998 ; EC, 1988). In our studies the mortality of animals were checked twice a day during the treatment period, and the data were recorded in the appropriate record sheet. The Table 1 shows the survival data.

Table 2. Survival of Rats in the 2-Year Feeding Studies

Parameters	Male	Female
Animals initially in study	50	50
Moribund and dead animals	22	23
Survival (No)	28	27
Survival (%)	56 %	54 %
Mean survival (days)	639.7	653.4

In spite of the *ad libitum* feeding, the percent survival of both sexes was above 50% at the end of 24th month, which is the important acceptance criteria of the carcinogenicity studies.

The survival graphs of male and female rats see in Fig. 1.

Figure 1. Survival of Male and Female Rats in 2-Year Carcinogenicity Study

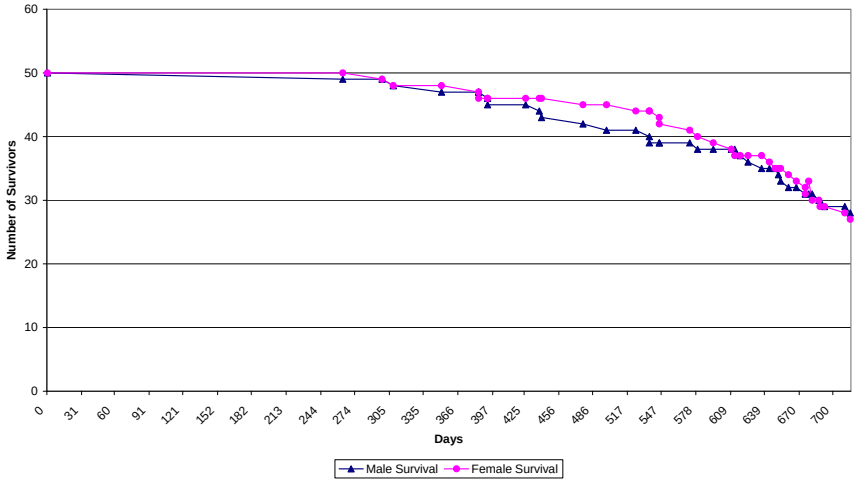

In Figure 1 we can see that survival is lower in male at around the 18th month of the study, which can be in connection with the high body weights. Table 3 shows the frequency of clinical symptoms observed during the study.

Table 3 Percentage Distribution of Clinical Signs Observed during the 2-year Period

Symptoms	**Percent of Animals**	
	Male	**Female**
Sudden Body Weight Lost	2	4
Swollen Limb	10	2
Wounds	34	36
Anaemia	0	0
Bloody Discharge	0	0
Mammary Gland Enlarged	6	52
Glaucoma	4	0
Limb Paralysis	2	2
Nodes	30	22
Activity Decrease	2	2
Alopecia	10	18
Ataxia	0	4

The observed clinical signs were in connection with aging of animals and with tumour development. The increase of findings in mammary gland of females is obvious.

Body weight and food consumption

The body weight and food consumption data of male and female rats see in Figures 2 and 3. The effect of *ad libitum* feeding manifested in the fast body weight gain in the first year of the study.

Figure 2. Mean Body Weight of Male and Female Rats

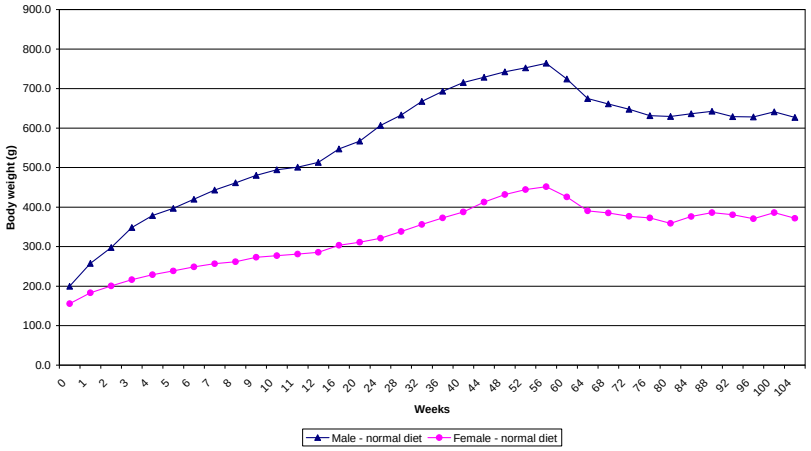

Figure 3. Food COnsumption of Male and Female Rats

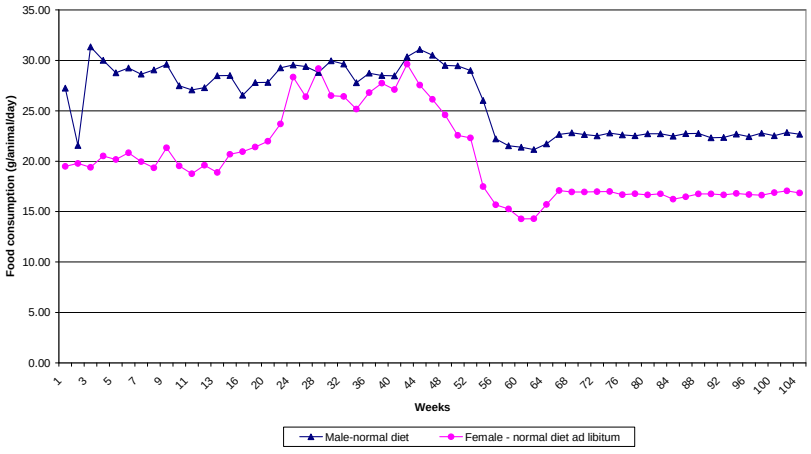

Haematology

The results of blood smear examinations at 12th and 18th months and at the end of the 24th month see in Table 3. The age-related change of the ratio of segmented cells and lymphocytes are very well demonstrated in this data set.

Table 4 Differential White Blood Cell Count in 2-Year Carcinogenicity Study

GROUPS		JU	ST	SE	EO	MO	BA	LY
		%	%	%	%	%	%	%
MALE								
Normal Diet	**MEAN**	0.00	0.04	15.53	1.06	1.28	0.00	82.09
12 Months	**SD**	0.00	0.29	9.63	1.44	2.26	0.00	10.31
	n	47	47	47	47	47	47	47
MALE								
Normal Diet	**MEAN**	0.00	0.05	18.15	0.87	0.05	0.00	80.87
18 Months	**SD**	0	0.32	10.05	1.2	0.32	0	10.01
	n	39	39	39	39	39	39	39
MALE								
Normal Diet	**MEAN**	0.00	0.29	33.50	1.21	1.00	0.00	64.00
24 Months	**SD**	0.00	0.71	14.53	1.75	1.92	0.00	14.57
	n	28	28	28	28	28	28	28
FEMALE								
Normal Diet	**MEAN**	0.00	0.00	17.50	1.00	0.29	0.00	81.21
12 Months	**SD**	0.00	0.00	9.73	1.37	0.82	0.00	9.66
	n	48	48	48	48	48	48	48
FEMALE								
Normal Diet	**MEAN**	0.00	0.14	23.45	1.91	0.32	0.00	74.32
18 Months	**SD**	0.00	0.51	13.09	4.29	0.86	0.00	14.55
	n	44	44	44	44	44	44	44
FEMALE								
Normal Diet	**MEAN**	0.00	0.00	34.44	1.56	1.11	0.00	63.00
24 Months	**SD**	0.00	0.00	18.75	4.62	2.31	0.00	20.00
	n	27	27	27	27	27	27	27

Remarks: Ju: juvenile, ST: stab cells, SE: segmented cells, EO: eosinophil cells, Mo: mono-cytes, BA: basophil cells, LY: lymphocytes

Pathology

Neoplastic alterations

With macroscopic examination alterations of tumorous origin (masses, foci, enlargements, etc.) could be observed in various organs of the animals. In the males hypophysis tumours could be detected most frequently, and the historical control data showed, that this type of tumour is typical to this strain. Tumour under the skin occurred in all groups too, but its incidence was lower, than of the hypophysis tumour. Tumours were observed in males with low frequency in the thymus, spinal column, omentum, kidneys, testes, prostate, abdominal lymph node, liver, mammary gland, Tumour-like alterations (enlargement, focus) occurred in males in the thyroid, salivary gland, lungs, adrenals, kidneys, spleen and in different lymph nodes as well. In the female animals tumour-like alterations occurred in the hypophysis, brain, lung, liver, adrenal gland, kidneys, in the genital organs, in the skin and mammary glands. These tumour-like alterations of females occurred sporadically with low incidence. Tumours caused moribund state or death sporadically with very low frequency in both sexes. The shock was indicated as cause of death with increased frequency in male animals, as well.

Non-neoplastic alterations

With the macroscopic examination a lot of non-neoplastic alterations could be observed in the different organs of the experimental animals. In the males dark-red, plethoric lungs, pulmonary oedema, heart dilatation, congested liver, pale liver, pale kidneys, atrophy of genitals, enlargement of testes and the thoracic cavity filled with serous liquide were observed. In the females pale liver, enlargement of spleen and

adrenals could be observed. The plethoric lungs and the pulmonary oedema occurred in less cases than in the males. Most of the non-neoplastic alterations were likely in connection with extermination and agony, or parts of them were age-related, or sporadical, toxicologically meaningless findings (congestion, discoloration, cysts, abscess etc.).

Organ Weight

The results of the organ weight measurements see in Table 5.

Table 5 Measured and Relative Organ Weights at the End of the 24th Month

Measured Organ Weights (G)						Relative Organ Weight Referred to Body Weight			
Group		**Body Weight**	**Brain**	**Liver**	**Spleen**		**Brain**	**Liver**	**Spleen**
Male	**Mean**	621.36	2.41	16.88	1.16	**Mean**	0.39	2.73	0.19
Normal Diet	**SD**	46.09	0.13	2.90	0.32	**SD**	0.03	0.55	0.05
24 Month	**n**	28	28	28	28	**n**	28	28	28
Group		**Body Weight**	**Brain**	**Liver**	**Spleen**		**Brain**	**Liver**	**Spleen**
Female	**Mean**	372.56	2.21	10.52	0.80	**Mean**	0.60	2.87	0.22
Normal Diet	**SD**	41.11	0.10	1.98	0.30	**SD**	0.07	0.73	0.08
24 Month	**n**	27	27	27	27	**n**	27	27	27

Histopathology

At the histological evaluation of the sections of different organs we observed different types of benign and malignant tumours, non-neoplastic hyperplastic lesions and non-neoplastic other lesions (degenerations, necrosis, inflammations etc.).

The main characteristics of malignant and benign neoplasms are demonstrated in the Table 6.

Table 6 Comparison of Benign and Malignant Neoplasms

Characteristic	Benign	Malignant
Growth rate	Slow	Rapid
Growth limits	Circumscribed	Unrestricted
Mode of growth	Expansion	Invasion
Differentiation	Good	Anaplastic
Stroma	Usually abundant	Usually scant
Metastasis	None	Frequent
Recurrence	Rare	Frequent

The most common causes of death were: pituitary adenoma, malignant (often generalized) tumours, chronic nephropathy, lung oedema and serious cystic degeneration of the adrenal glands.

Pituitary adenoma

Pituitary adenomas are well-delineated masses that compress the surrounding parenchyma. The neoplastic cells are arranged in solid sheets or compact branching cords. The vascular pattern may be more or less evident, but large neoplasms often have angiectasis, cyst-like lesions and/or haemorrhage. According to the historical literature data the pituitary adenomas are common in Charles River CD rats. The incidence varies from 0 % to 90 % in old male and female animals.

The other malignant tumours

In this study – in accordance with the historical data - pituitary adenomas were the most common tumours. Undifferentiated sarcoma in the heart, undifferentiated carcinoma in the skin, fibrosarcoma in the skin, intestines and prostate, follicular carcinoma in the thyroid gland, astrocytoma in the brain, adenocarcinoma in the lung, Leydig-cell tumour in the testes were detectable only sporadically.

The malignant tumours which caused death of animals were the fibrosarcoma, and adenocarcinoma, which were infrequent in both males and females.

Benign tumours

The most common benign tumour was in this study the mammary gland adenoma in the female animals. The other types of benign neoplasms, fibroma in the mammary gland, skin, thoracic or abdominal cavity, fibro-adenoma and lipoma in the skin, adenoma in the thoracic cavity, adrenal gland, thyroid gland, thymoma in the thymus, pheochromocytoma in the adrenal gland, myxoma and adenoma in the uterus, seminoma in testes had generally low frequency.

Non-neoplastic hyperplastic lesions

At the histological evaluation of different organs of experimental animals we observed non-neoplastic hyperplastic lesions (hyperplastic nodules and bile duct hyperplasia in the liver, C-cell hyperplasia in the thyroid gland, islet-cell hyperplasia in the pancreas, cystic hyperplasia in the seminal vesicle) as well.

Hyperplastic nodules in the liver were rare and occurred in the control animals as well. The foci of cellular alteration belonged mainly to hyperplasias, that are perceived to be secondary, non-neoplastic responses to degenerative changes of the liver. Some focus of cellular alteration was basophilic, and eosinophilic character. No compressions of surrounding parenchyma or higher incidence of mitotic figures were seen.

Bile duct hyperplasia is a common aging lesion in control rats often accompanied by perilobular fibrosis. The C-cell hyperplasia in the thyroid gland, the cystic hyperplasia in the seminal vesicle and the islet-cell hyperplasia in the pancreas were detectable only sporadically. Table 7 and Table 8 show the incidence of tumours in histopathological findings, which can serve as a historical control data in evaluation of chronic and carcinogenicity studies performed under similar conditions. Table 9 shows the overall incidence of benign and malignant tumours and hyperplastic findings by groups and sex at the fatal death, moribund animals and at the terminal necropsy.

Discussion

The stipulation of use and circulation of agricultural chemicals, especially of pesticides is authority registration. The organic part of the registration documentation is the estimation of the carcinogenic effect of the product on the basis of the 2-year carcinogenicity study on rats or mice. In evaluation of this type of study the caloric intakes are now recognized to be important uncontrolled variables. Furthermore the use of historical control data during the evaluation is essential and recommended by the internationally accepted guidelines (OECD, 1981; EC, 1988; US EPA, 1988; FDA, 1996).

Table 7 Summary Incidence of Histopathological Findings (Fatal Death or Moribund Condition) (Tumours)

HISTOPATHOLOGICAL FINDINGS PER ORGANS	GROUP	Normal Diet		Normal Diet	
	SEX	Male		Female	
	ANIMAL NR / GROUP (Died)	22		23	
	SUM	Σ	%	Σ	%
PITUITARY	adenoma	7	32	13	57
MAMMARY GLAND	adenoma	-	-	2	9
	fibroma	1	5	-	-
	adenocarcinoma	-	-	5	22
SKIN	fibroma	1	5	1	4
	carcinoma	1	5	2	9
	fibrosarcoma	-	-	1	4
TUMOUR in the thoracic or abdominal cavity	adenoma	-	-	1	4
GENERALIZED TUMOUR	myeloma malignum	1	5	-	-
	sarcoma polymorphocellulare	-	-	-	-
	fibrosarcoma	1	5	-	-
	carcinoma	1	5	-	-
LUNG	adenocarcinoma	1	5	-	-
HEART	sarcoma	1	5	-	-
ADRENAL GLAND	cortical adenoma	-	-	2	9
THYROID GLAND	follicular adenoma	-	-	1	4
BRAIN	astrocytoma	-	-	2	9
TESTES	seminoma	1	5	-	-

Table 8 Summary Incidence of Histopathological Findings (Terminal Necropsy of Survivors) (Tumours)

HISTOPATHOLOGICAL FINDINGS PER ORGANS	GROUP	Normal Diet		Normal Diet	
	SEX	Male		Female	
	ANIMAL NR / GROUP (Survival)	28		27	
	SUM	Σ	%	Σ	%
PITUITARY	adenoma	5	18	18	67
MAMMARY GLAND	adenoma	-	-	6	22
	fibroma	1	4	-	-
	adenocarcinoma	-	-	1	4
SKIN	lipoma	1	4	-	-
	fibro-adenoma	-	-	5	19
	carcinoma	-	-	1	4
TUMOUR in the thoracic or abdominal cavity	adenoma	2	7	1	4
INTESTINE	fibrosarcoma	1	4	-	-
ADRENAL GLAND	pheochromocytoma	4	14	-	-
THYROID GLAND	follicular adenoma	4	14	1	4
	follicular carcinoma	2	7	1	4
TESTES	seminoma	2	7	-	-
	Leydig-cell Tumour	2	7	-	-
PROSTATE	fibrosarcoma	1	4	-	-
UTERUS	adenoma	-	-	1	4
	myxoma	-	-	1	4

Table 9 Overall Incidence of Benign and Malignant Tumors

LESIONS	Fatal Death and Moribund		Terminal Necropsy	
	M	**F**	**M**	**F**
No. of animals	22	23	28	27
pituitary adenoma	7	13	5	18
bening tumours	3	5	16	15
malignant tumours	6	10	4	3
tumours (total)	9	15	20	18
non-neoplastic hyperplasia	4	2	13	6
pituitary adenoma/animal	0.32	0.57	0.18	0.67
benign tumours / animal	0.14	0.22	0.57	0.56
malignant tumours / animal	0.27	0.43	0.14	0.11
tumours (total) / animal	0.41	0.65	0.71	0.67
non-neoplastic hyperplasia / animal	0.18	0.09	0.46	0.22

Remark: M = Male
F = Female

In our study we observed slightly increased mortality of male rats at around the 18th month of the study, which can be in connection with the rapid body weight gain of young male animals. In spite of the *ad libitum* feeding, the percent survival of both sexes was above 50% at the end of 24th month, which is the important acceptance criterion of the carcinogenicity studies (FDA, 1996).

The mean body weight and food consumption data are summarized as well as the haematological findings and organ weight data. These data well demonstrated the age-related changes of the parameters of experimental animals (Karsai et al, 1993; Gál, 1999).

On the basis of the pathological and histopathological results the most common causes of death observed during the study were the pituitary

adenoma, malignant (often generalized) tumours, chronic nephropathy, lung oedema and serious cystic degeneration of the adrenal glands.

The pituitary adenoma was observed with the highest frequency, which is in line with the literature and proved strain-related alteration. (Charles River 1988) The mammary gland adenoma in female animals was the second very frequent neoplastic alteration. The incidence and frequency of neoplastic changes are reported in details, so these can be used as historical control data during the evaluation of carcinogenicity studies performed in the investigated rat strain under similar conditions.

References

Berg J.W. 1975. Can nutrition explain the pattern of international epidemiology of hormone-dependent cancer? *Cancer Res.* **35**. 3345-3350.

Chambers, J. E. and Yorbrough, J. D. (ed.) 1982. Effects of Chronic Exposures to Pesticides on Animal Systems. Raven Press, New York.

Costa M. 1980. Metal Carcinogenesis Testing. The Human Press Inc. Clifton, New Yersey.

Charles River 1988. Crl:CD Br Rat. Collection of Charles River Lab. Publications. Charles River, Deutschland.

De Brabander, M., Mareel, M., De Ridder L. 1979. Cell Movement and Neoplasia. Janssen Research Foundation, Beerse, Belgium

EC 1988. Commission Directive 88/302/EEC of 18 November 1987 adapting to technical progress for the ninth time Council Directive 67/548/EEC on the approximation of the laws, regulations and administrative provisions relating to the classification, packaging and labelling of dangerous substances. B.32. Carcinogenicity test

EC 1991. Commission Directive 91/414/EEC of 19 August 1991. The Plant Protection Products Directive (OJ L230, ISSN 0378 6978)

EC 1997. Application of the Uniform Principles ensures that authorisations issued in all Member States are assessed to the same standards OJ L265, p.87.

FDA 1996. ICH Harmonised Tripartite Guideline S1A, Guideline on the Need for Carcinogenicity Studies of Pharmaceuticals.

Gál, T. (ed) 1999. Állatorvosi klinikai laboratóriumi diagnosztika. SÍK Kiadó Budapest.

Garfinkel, L.E. 1985. Overweight and cancer. *Ann. Intern. Med*. **103**. 1034-1036.

Girdwood, R.H. (ed) 1974. Blood Disorders Due to Drugs and Other Agents. Excerpta Medica, Amsterdam.

Growing, N.F.C. 1980. A Colour Atlas of Tumour Histopathology. Wolfe Medicinal Publications Ltd. London

Kardeván, A. 1976. A háziállatok kórbonctana. Mezőgazdasági Kiadó, Budapest.

Karsai, F., Vörös K., 1993. Állatorvosi belgyógyászat. Mezőgazda Kiadó, Budapest.

Kiss, I. 1997. Toxikológia. Veszprémi Egyetemi Kiadó, Veszprém.

Kritchevsky, D., Welch, C.B. and Klurfeld, D.M., 1989. Response of mammary tumours to caloric restriction for different time periods during the promotion phase. Nutr Cancer;12. 259-269.

Lavik, P.S. and Baumann, C.A., 1943. Further studies on tumour-promoting action of fat. *Cancer Res*. **3.** 749-756.

Lyon, J.L., Mahoney, A.W., West, D.W., Gardner, J.W., Smith, K.R., Sorenson, A.W. and Stanish, W. 1987. Energy intake: its relationship to colon cancer. *J. Natl. Cancer. Inst*. **78**. 853-861.

OECD, 1981. Guidelines for Testing of Chemicals No. 452, Carcinogenicity Study.

Papolcsy, A. 1975. A tüdő jóindulatú daganatai. Medicina Budapest.

Potter, V.R. 1945. The role of nutrition in cancer prevention. Science;101. 105-109.

Resnik, H. and Schüller M., 1983. Comparative Respiratory Tract Carcinogenesis. CRC Press, New York.

Ross, M.H. and, Bras, G. 1971. Lasting influence of early caloric restriction on prevalence of neoplasms in the rat. *J. Natl. Cancer. Inst.* **47**. 1095-1113.

Tannenbaum, A., 1959. Nutrition and cancer. In: Homburger, F., (ed) The physiopathology of cancer. Hoeber-Harper Inc, New York. 517-562.

U.S. EPA, 1998, Office of Prevention, Pesticides and Toxic Substances, Health Effects Test Guidelines, Carcinogenicity. (OPPTS 870.4200)

Vena, J.E., Graham, S., Zielezny, M., Swanson M.K., Barnes R.E. and Nolan J., 1985. Lifetime occupational exercise and colon cancer. *Am J Epidemiol*. **122**. 357-365.

Wallace A.H., (ed) 1989. Principles and Methods of Toxicology. Edited by A., Raven Press New York.